Sedimentary Geology 222 (2009) 181–206

Contents lists available at ScienceDirect

Sedimentary Geology

journal homepage: www.elsevier.com/locate/sedgeo

Facies and climate/environmental changes recorded on a carbonate ramp: A sedimentological and geochemical approach on Middle Jurassic carbonates (Paris Basin, France)

Benjamin Brigaud [a,b,*], Christophe Durlet [a], Jean-François Deconinck [a], Benoît Vincent [c], Emmanuelle Pucéat [a], Jacques Thierry [a], Alain Trouiller [b]

[a] Université de Bourgogne, UMR CNRS 5561 Biogéosciences, 6 bd Gabriel, 21000 Dijon, France
[b] Andra, 1-7 rue Jean Monnet, 92298 Châtenay-Malabry Cedex, France
[c] Andra, Laboratoire de Recherche Souterrain de Meuse/Haute-Marne, Route Départementale 90—BP 9, 55290 Bure, France

ARTICLE INFO

Article history:
Received 30 April 2009
Received in revised form 31 July 2009
Accepted 2 September 2009

Keywords:
Carbonate
Oxygen isotope
Stratigraphy
Climate
Middle Jurassic
Paris Basin

ABSTRACT

A detailed sedimentological, geochemical and mineralogical study is carried out on the Early Bajocian to Early Callovian (Middle Jurassic) limestones of the Paris Basin. Objectives are to document and explain the facies changes in the context of the climate/environmental evolution at the NW European scale. Deposits include 18 lithofacies which are stacked into 10 third-order depositional sequences. At a greater time scale, 4 biosedimentary packages are distinguished by their allochems associations. (1) An intracratonic carbonate environment with coral reefs and crinoid-rich facies is typical of the Early Bajocian. (2) A major facies change occurred at the Early/Late Bajocian transition with a shift from crinoid- and coral-rich facies to ooid-rich facies. During the Late Bajocian, a southward-dipping ooid ramp with successive progradational trends was emplaced. (3) A large lagoon protected by ooid shoals developed during the Bathonian in a muddy ramp setting. (4) At the Bathonian/Callovian boundary, a second major change occurred with the lagoonal facies being superseded by an ooid-bioclastic (crinoids, corals) ramp associated with a waning of carbonate productivity (retrogradational trend). Our geochemical study including a compilation of bibliographic data allows us to refine the existing sea surface palaeotemperature pattern. A cooling from the latest Early Bajocian to the Late Bajocian and a subsequent warming from the earliest Callovian to the Early/Middle Callovian transition are described using a proxy of sea surface temperatures. Together with $\delta^{13}C$ and mineralogical data, our new $\delta^{18}O$ values suggest a palaeo-climatic/palaeo-environmental control of facies in this shallow carbonate ramp environment.

1. Introduction

The Middle Jurassic carbonate formations of the eastern part of the Paris Basin form the basement of the natural clay barrier chosen by the French National Agency for Radioactive Waste Management (Andra) as a target for a laboratory aiming to study the deep disposal of radioactive waste. The carbonate architecture and lithological changes are of primary importance for Andra hydrologists seeking to better constrain the local hydrological system, which is mainly controlled by the geometry and facies properties of these carbonate formations. The pioneering studies of Middle Jurassic carbonate bodies from Burgundy (Purser, 1975) have been supplemented by numerous studies in this part of the Paris Basin. They focus on facies analysis and depositional reconstructions from well-biostratigraphically constrained outcrops of Early Bajocian (Durlet and Thierry, 2000; Durlet et al., 2001b; Guillocheau et al., 2002), Late Bathonian/Callovian (Floquet et al., 1989; Laville et al., 1989; Javaux, 1992; Gaumet et al., 1996). However synthetic facies evolutions of the whole interval including geochemical data are not available. Well-log correlations applied at a multi-basin scale (England, Paris Basin and South-East France Basin), were carried out on the Late Bathonian/Callovian interval (Garcia et al., 1996a; Gaumet et al., 2001), or the Jurassic interval (Jacquin et al., 1998). Those studies identify eustasy as the dominant factor of carbonate architecture and production in the Paris Basin. However the possible influence of climatic and seawater-chemistry changes on facies is poorly documented in the eastern Paris Basin carbonate environments.

The main objectives are to document and explain the main facies changes in the Middle Jurassic deposits of the eastern Paris Basin. This paper is based on a multidisciplinary approach including facies analysis, stable isotope chemistry and clay mineralogy within a biostratigraphic and sequence stratigraphic framework. The main results are

* Corresponding author. Université de Bourgogne, UMR CNRS 5561 Biogéosciences, 6 bd Gabriel, 21000 Dijon, France.
E-mail address: benjamin.brigaud@u-bourgogne.fr (B. Brigaud).

0037-0738/$ – see front matter © 2009 Elsevier B.V. All rights reserved.
doi:10.1016/j.sedgeo.2009.09.005

used to discuss the relative influences of eustatic, tectonic and climatic/environmental factors on the main facies changes.

Analyses are carried out on Middle Jurassic outcrops and cored boreholes in the eastern Paris Basin (between Langres and Nancy). A detailed schematic transect representing the carbonate architecture is compiled to characterize the depositional environments, to represent the allochem associations and their lateral and vertical patterns and finally to propose synthetic facies and depositional environment changes during the Middle Jurassic interval. An oxygen isotopic study is conducted to better constrain the palaeotemperature curve of this period, which is poorly constrained compared to the Early Jurassic (Dera et al., 2009a) or the Late Jurassic (Wierzbowski, 2002, 2004; Brigaud et al., 2008). Isotopic data are then used to test the possible influence of climatic and seawater-chemistry changes on biofacies. Clay mineral assemblages are also analysed to evaluate and specify the possible climatic control of their distribution in this part of the Paris Basin.

2. Geological setting

Located at subtropical latitudes (25–30° N) during Bajocian–Callovian times, the Paris Basin was covered by an epicontinental sea open to the Atlantic, Tethys and Northern Oceans (Fig. 1, Thierry, 2000). On a broad scale, North West Europe was an archipelago composed of eroded Hercynian massifs and the study area lay between the Central Armorican, London-Brabant and Bohemian Massifs.

Purser (1975) recognized biosedimentary packages – previously called *lithoclines* – in the Middle Jurassic limestones of the eastern Paris Basin which are described below:

Early Bajocian sediments, composed mostly of bioclastic calcarenites and coral buildups – the *Calcaires à polypiers* (Fig. 2) – were deposited on a vast carbonate environment extending over almost all of the Paris Basin (Fig. 2, Durlet et al., 2001b; Guillocheau et al., 2002).

Echinoderms (mainly crinoids) and bivalves associated with peloids are the main allochems of this carbonate formation (Ferry et al., 2007).

At the Early/Late Bajocian boundary, an abrupt lithological change occurred with the appearance of terrigenous components above an encrusted bored surface corresponding to the 'Vesulian Unconformity' (Fig. 2, Durlet and Thierry, 2000). This carbonate crisis is recognized throughout the north-western Tethyan domain (Jacquin et al., 1998; Piuz, 2004). The mixed terrigenous/carbonate sedimentation continued into the Late Bajocian in the south-western part of the study area and Burgundy with the deposition of the *Ostrea acuminata* Marls (Fig. 2). In the north-eastern part of the study area, marly sedimentation (*Marnes de Longwy and Oolite à Clypeus ploti*) and calcarenite sedimentation (*Oolite miliaire inférieure et supérieure*) alternated. Carbonate episodes correspond to the progradation of sedimentation along an ooid ramp dipping gently southward from the London-Brabant landmass (Guillocheau et al., 2002).

During the Bathonian, a carbonate ramp with diversified facies developed across the Paris Basin (Purser, 1975, 1989; Ferry et al., 2007). Three main depositional environments are recognized (Fig. 2): (1) a typical shoal fringe with abundant ooids, peloids, bivalve, bryozoan and gastropod bioclasts (*Oolite Blanche* and *Oolite de Fréville*); (2) a protected lagoon behind the oolitic shoal with fine sedimentation characterized by mudstones with oncoids and benthic foraminifera, wackestones/packstones with oncoids, and peloidal grainstones (*Calcaires de Chaumont* and *Calcaires de Neufchâteau*); (3) an intertidal to supratidal area with ephemeral tide-related subaerial exposures, characterized by laminated mudstone (stromatolites) with fenestral structures, mud cracks and vadose cementations (Purser, 1975; Javaux, 1992).

The Early Callovian carbonate formation displays mostly ooids, bryozoans, echinoderms and bivalve-rich bioclastic sediments (Javaux, 1992) and is restricted to the south-western part of the study area (*Pierre de Dijon-Corton* and *Pierre de Ladoix*; Fig. 2). These shallow marine carbonates correspond laterally to the north to marly, open marine deposits (*Argiles de la Woëvre*). Thus, due to this lateral variation, a second abrupt lithological change occurred at the Late Bathonian/Early Callovian boundary in the north-east, and later at the Early Callovian/Middle Callovian boundary in the south-west.

3. Materials and methods

3.1. Facies analysis

This study is based on the detailed examination of 37 outcrop sections between Langres and Nancy, and of four cores (EST210, EST433, HTM102 and L.LI.CD.1; Fig. 1). Three outcrops and five boreholes from previous works are used to complete the descriptions (Faber, 1957; Guillocheau et al., 2002). Outcrop sections and cores were logged in detail and microfacies were analysed on a total of 388 thin-sections. The proportion of facies components (bioclasts and non-bioclastic elements) is estimated from 266 thin sections from EST210, EST433, HTM102 and L.LI.CD.001 cores. This semi-quantitative estimation is calibrated by point-counting analyses of 10 representative thin-sections using the Jmicrovision Image (Roduit, 2008) analysis system with a minimum of 200 counts per section. Facies classification and their environmental interpretation are based on texture, bioclasts and non-bioclastic elements, sedimentary structures, bioturbations and hydrodynamism (Purser, 1980; Purser, 1983; Tucker and Wright, 1990; Flügel, 2004). Early cements are observed under a cathodoluminescence microscope coupled to a digital camera in order to characterize the early cementation processes and their origin.

3.2. Geochemical analysis

In order to reconstruct Middle Jurassic seawater temperatures, 59 *Trichites* shells, 50 oyster shells and 3 belemnites rostra were recovered from eastern Paris Basin outcrops (10 outcrops and 1 core; see Appendix A for location). Each Low Magnesium Calcite (LMC) shell (0.5 cm to 2 cm thick) was sectioned, polished and investigated using cathodoluminescence (CL) microscopy to identify diagenetic recrystallisations. Luminescent and non-luminescent areas of each shell and rostrum were accurately mapped to sample exclusively the well preserved non-luminescent areas for isotopic analyses. After CL studies, 50 *Trichites* shells, 41 oyster shells and 3 belemnites guards were selected and micro-drilled from non-recrystallized parts for isotopic investigations. The carbon and oxygen isotope compositions of 197 micro-drilled parts from the 94 well-preserved bivalves and belemnites (on average more than two sub-samples per bivalve shell or belemnite guard) were analysed at the Leibniz Laboratory for Radiometric Dating and Stable Isotope Research, Kiel (Germany). Calcite powders were reacted with 100% phosphoric acid at 75 °C using a Kiel III online carbonate preparation line connected to a ThermoFinnigan 252 mass-spectrometer. All isotopic values are reported in the standard δ-notation in per mil relative to V-PDB (Vienna Pee Dee Belemnite) by assigning a $\delta^{13}C$ value of +1.95‰ and

Fig. 1. A—Location of the study outcrops and boreholes on a simplified geological map of the eastern Paris Basin. B—Location of the study area on palaeogeographic reconstruction (from Purser, 1975; Enay and Mangold, 1980; Thierry, 2000) with locations of isotope study sites from the literature: Bulgaria (Metodiev and Koleva-Rekabova, 2008); England (Anderson et al., 1994; Podlaha et al., 1998; Jenkyns et al., 2002; Price and Page, 2008); Germany (Podlaha et al., 1998); Poland (Wierzbowski and Joachimski, 2007); Portugal (Jenkyns et al., 2002); Russia (Podlaha et al., 1998; Riboulleau et al., 1998) and Scotland (Jenkyns et al., 2002; Nunn et al., 2009). C—Palaeogeographic map of France (modified from from Purser, 1975; Enay and Mangold, 1980).

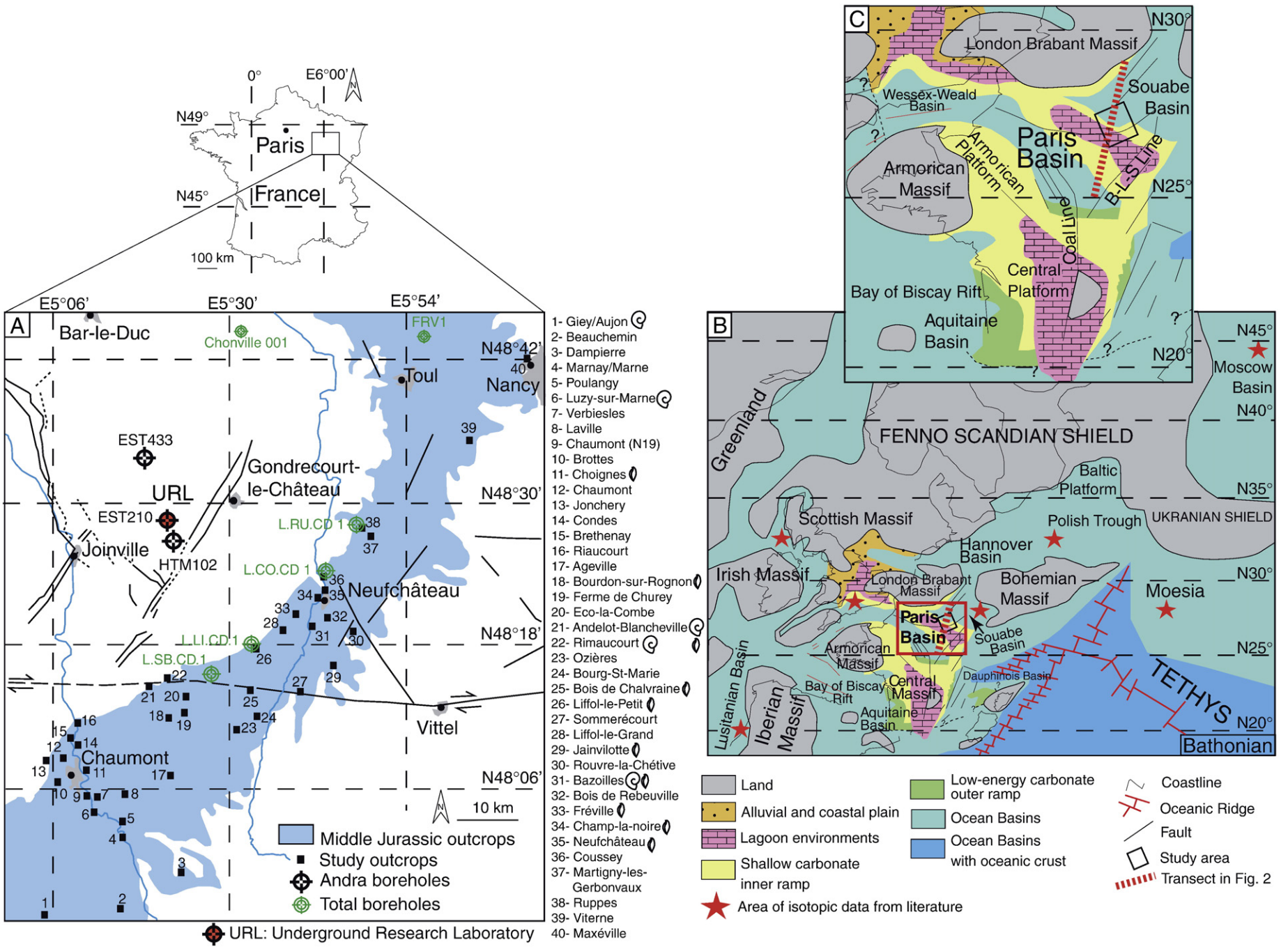
A
B
C
0°
E6°00'
N49°
N45°
Paris
France
100 km
E5°06'
E5°30'
E5°54'
Bar-le-Duc
Chonville 001
FRV1
N48°42'
Toul
Nancy
40
EST433
39
Gondrecourt-
le-Château
URL
N48°30'
EST210
L.RU.CD 1
38
37
Joinville
HTM102
L.CO.CD 1
36
Neufchâteau
34
35
33
32
28
31
30
N48°18'
L.LI.CD 1
26
L.SB.CD.1
22
27
29
21
20
25
18
19
24
23
16
15
14
12
Chaumont
13
11
17
Vittel
N48°06'
10
9
7
8
6
5
4
3
2
1
10 km
Middle Jurassic outcrops
Study outcrops
Andra boreholes
Total boreholes
URL: Underground Research Laboratory
1- Giey/Aujon
2- Beauchemin
3- Dampierre
4- Marnay/Marne
5- Poulangy
6- Luzy-sur-Marne
7- Verbiesles
8- Laville
9- Chaumont (N19)
10- Brottes
11- Choignes
12- Chaumont
13- Jonchery
14- Condes
15- Brethenay
16- Riaucourt
17- Ageville
18- Bourdon-sur-Rognon
19- Ferme de Churey
20- Eco-la-Combe
21- Andelot-Blancheville
22- Rimaucourt
23- Ozières
24- Bourg-St-Marie
25- Bois de Chalvraine
26- Liffol-le-Petit
27- Sommerécourt
28- Liffol-le-Grand
29- Jainvilotte
30- Rouvre-la-Chétive
31- Bazoilles
32- Bois de Rebeuville
33- Fréville
34- Champ-la-noire
35- Neufchâteau
36- Coussey
37- Martigny-les-
Gerbonvaux
38- Ruppes
39- Viterne
40- Maxéville
London Brabant Massif
Wessex-Weald
Basin
Souabe
Basin
Armorican
Platform
Paris
Basin
Armorican
Massif
B-L-S Line
N25°
Coal Line
Central
Platform
Bay of Biscay Rift
Aquitaine
Basin
N20°
N30°
N45°
Moscow
Basin
N40°
Greenland
FENNO SCANDIAN SHIELD
Baltic
Platform
N35°
Scottish Massif
Polish Trough
UKRANIAN SHIELD
Hannover
Basin
Irish Massif
London Brabant
Massif
Bohemian
Massif
Moesia
N30°
Paris
Basin
Souabe
Basin
Armorican
Massif
N25°
Lusitanian Basin
Iberian
Massif
Bay of Biscay
Rift
Central
Massif
Dauphinois Basin
TETHYS
Aquitaine
Basin
N20°
Bathonian
Land
Alluvial and coastal plain
Lagoon environments
Shallow carbonate
inner ramp
Area of isotopic data from literature
Low-energy carbonate
outer ramp
Ocean Basins
Ocean Basins
with oceanic crust
Coastline
Oceanic Ridge
Fault
Study area
Transect in Fig. 2

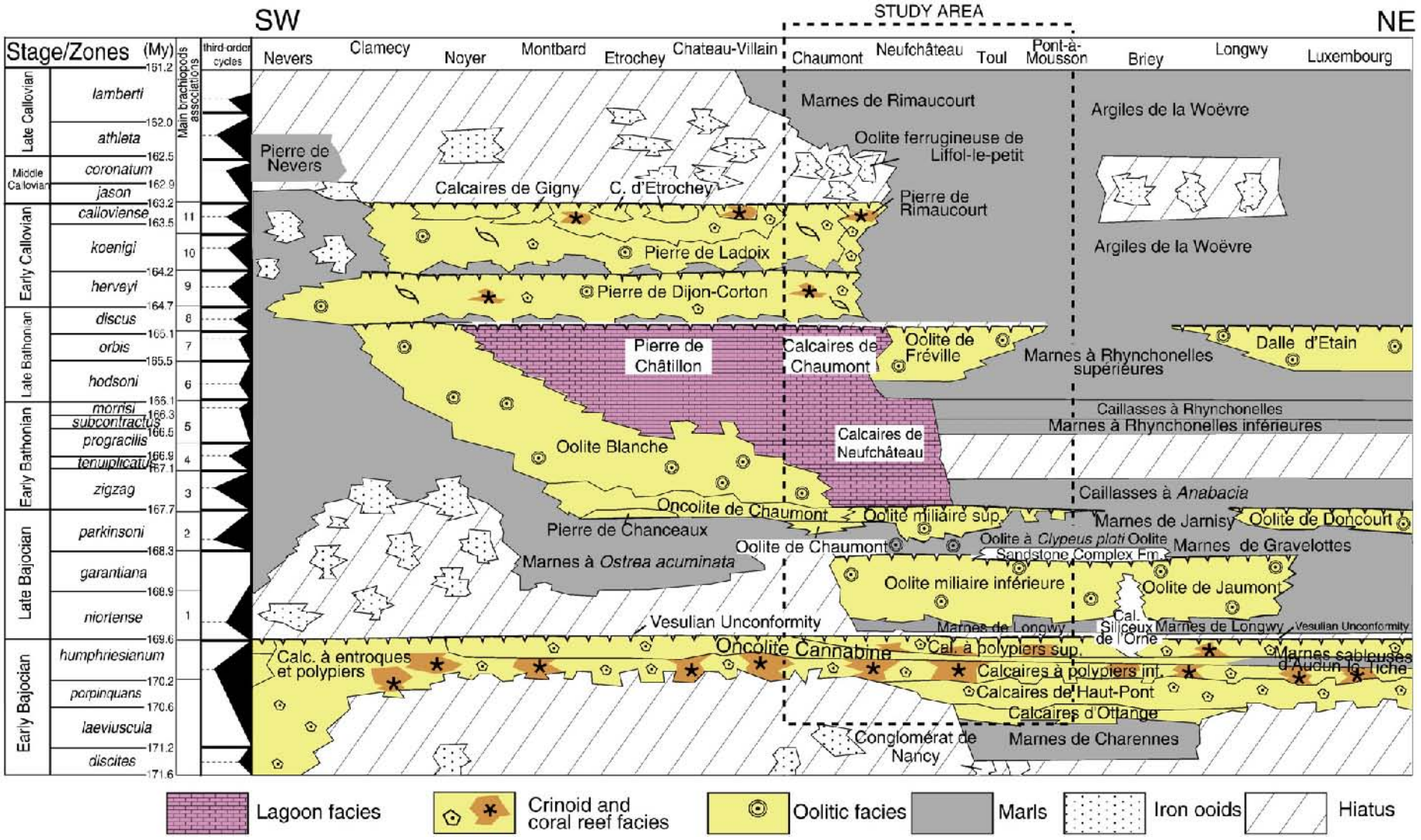

Fig. 2. Schematic lithostratigraphic illustration of a north–east–south-west transect (modified from Contini, 1968; Thierry et al., 1980). Biostratigraphic ammonite zonation and ages from Gradstein et al. (2004). Previous biostratigraphic studies based on brachiopod and ammonite faunas are used to constrain the timing of facies evolution (Thierry et al., 1980; Mangold et al., 1994; Garcia et al., 1996b; Courville and Raffray, 2007). Additional brachiopods and ammonites were collected to improve the pre-existing dating based on brachiopod associations (Garcia et al., 1996b). Main brachiopod associations for the Bajocian–Callovian intervals corresponding to third-order maximum flooding surface in the Paris Basin (Garcia et al., 1996b; Hardenbol et al., 1998): 1—*Lissajousithyris matisconensis* association, 2—*Ferrythyris ferryi* and "*R.*" *edwarsi* association, 3—*Rocheityris curvata* and *Globirhynchia sp.* association, 4—*Tubithyris globata* association, 5—*Burmirhynchia cf. multiplicata* association, 6—*Lotharingella woevrica* and *Kallirhynchia concinna* association, 7—*B. thierachensis*, *B. proteiformis*, *Digonella digona* and *Kutchirhynchia cf obseleta* association, 8—*Eudesia multicostata* and *B. elegantula* association, 9—*Digonella divionensis, Lotharingella gremifera, L. leedsi* and *Ornithella sp1.* association, 10—*Septaliphoria mourdoni* association, 11—*Kallirhynchia* sp. and *Ornithella* sp. association.

Table 1
Lithofacies descriptions.

Lithofacies	Non-bioclastic components	Bioclastic components	Sedimentary and biogenic structures	Sorting and grain size	Energy and depositional environment	General environmental interpretation
F1—marls with abundant quartz and bivalves	Quartz (C), wood fragments (R)	Bivalves (F), brachiopods (F), crinoids (F), sponges (F), ammonites (F)	Abundant bioturbation	Quartz ~100 μm well sorted	Very low energy lower offshore	Outer-ramp Paleodepth > 50 m
F2a—oncoid wackestone/packstone	*Nubecularia* oncoids (A), ooids (R), pellets (R)	Foraminifera (F), bivalves (F), crinoids (F), ammonites (F), corals (C)	50 cm planar bedding bioherms (<2 m thick and <3 m lateral extend)	~100 μm to 0.5 cm poorly sorted	Low to moderate energy upper offshore	Mid-ramp environment Paleodepth—30–50 m
F2b—bivalve/echinoderm wackstone/packstone	Pellets (C), quartz (R)	Bivalves (A), miliolina (C), echinoids (C), brachiopods (C), corals (R))	10 cm to 1 m planar bedding, (HCS), bioturbation	Poorly sorted	Low to moderate energy upper offshore	
F2c—ooid/crinoid Wackestone/Packstone	Ooids (C), intraclasts (F)	Crinoids (A), bivalves (F); brachiopods (F); sponges (F), echinoids (R), coral (R))	Tempestite (HCS)	Pebbles ~5 mm to 5 cm very poorly sorted	Low to moderate energy upper offshore (storms)	
F3a—radial ooid packstone/grainstone	Radial ooids (A)	Bivalves (R), crinoids (R), brachiopods (R), bryozoan (R)	Cross bedding	500 μm; very well sorted	Moderate energy, wave dominated, shoreface	Inner ramp environment (shoal and reef)
F3b—concentric ooid grainstone	Concentric ooids (A), superficial ooids (R)	Bivalves (F), coral debris (C), brachiopods (R), gastropods (R), intraclast (F)	Cross bedding	500 μm to 1 mm; very well sorted	High energy, wave dominated, shoreface	Paleodepth <30 m
F3c—micritic ooid grainstone	Micritic ooids (A)	Bivalves (F), green algae (R)	Cross bedding	500 μm to 1 mm; very well sorted	High energy, wave dominated, shoreface	
F3d—superficial ooid grainstone	Superficial ooids (A), oncoids (F)	Bivalves (A), crinoids (C)	Cross bedding	250 μm to 5 mm poorly sorted	High energy, wave dominated, shoreface	
F3e—bioclastic ooid grainstone	Ooids (A)	Bivalves (A), crinoids (C), bryozoan (C), intraclasts (F)	Cross bedding	50 μm to 5 mm; very poor sorted	High energy, wave dominated, shoreface	
F3f—bioclastic peloidal grainstone	Peloids (A), nubecularia oncoids (R)	Echinoids (A), crinoids (A), bivalves (A), coral debris (F)	Cross bedding	250 μm to 3 mm; moderately sorted	High energy, wave dominated, shoreface	
F3g—coral bioconstructions (boundstone)		Lamellar, massive, ramose phaceloid corals (A), bivalves (F)	Bioherms and biostromes (2–10 m thick and 2–20 m lateral extent)		High energy, wave dominated, shoreface	
F3h—crinoid/packstone grainstone	Peloids (C)	Crinoids (A), brachiopods (C); bryozoans (C)	Cross bedding	1 mm; well sorted	High energy, wave dominated, shoreface	
F4a—peloidal/foraminiferal Mudstone/Packstone	Oncoids (F), peloids (A), ooids (F), intracalsts (C)	Foraminifera (C), bivalves (C), echinoderms (R), *Cayeuxia* (C)	Planar bedding	50 μm to 1 cm very poorly sorted	Low to moderate energy protected environments	Inner ramp lagoon Paleodepth <30 m
F4b—oncoid–peloid packstone/grainstone	Intraclasts (C), ooids (C), pellets (C)	Ooids (C), foraminifera (C)	Cross bedding	50 μm to 5 cm very poor sorted	Low to moderate energy protected environments	
F4c—pellet grainstone/packstone	Pellets (A), wood fragments (R)	Bivalves (C), foraminifera (C), *Cayeuxia* (C)	Planar and cross bedding	30–10 μm well sorted	Low to moderate energy protected environments	
F5a micritic algal mudstone/packstone	Peloids (F), oncoids (C)	Bivalves (R)	Peloidal structures microbial laminae birdseyes, root traces	Poorly sorted	Low energy shoreface	Inner ramp supratidal Paleodepth <5 m
F5b—oncoid-bioclastic grainstone/rudstone	Pellet (C), intraclasts (R/F), peloids (F), oncoids (C)	Foraminifera (C/A), bivalves (A) gastropods (A), *Cayeuxia* (C)	Birdseyes, stalactitic cements	100 μm to 2 cm very poorly sorted	High energy, foreshore, beach	
F5c—lignite					Very low energy backshore	

R = rare: < 10%; C = common: 10–20%; F = frequent: 20–30%; A = abundant: > 50‰.

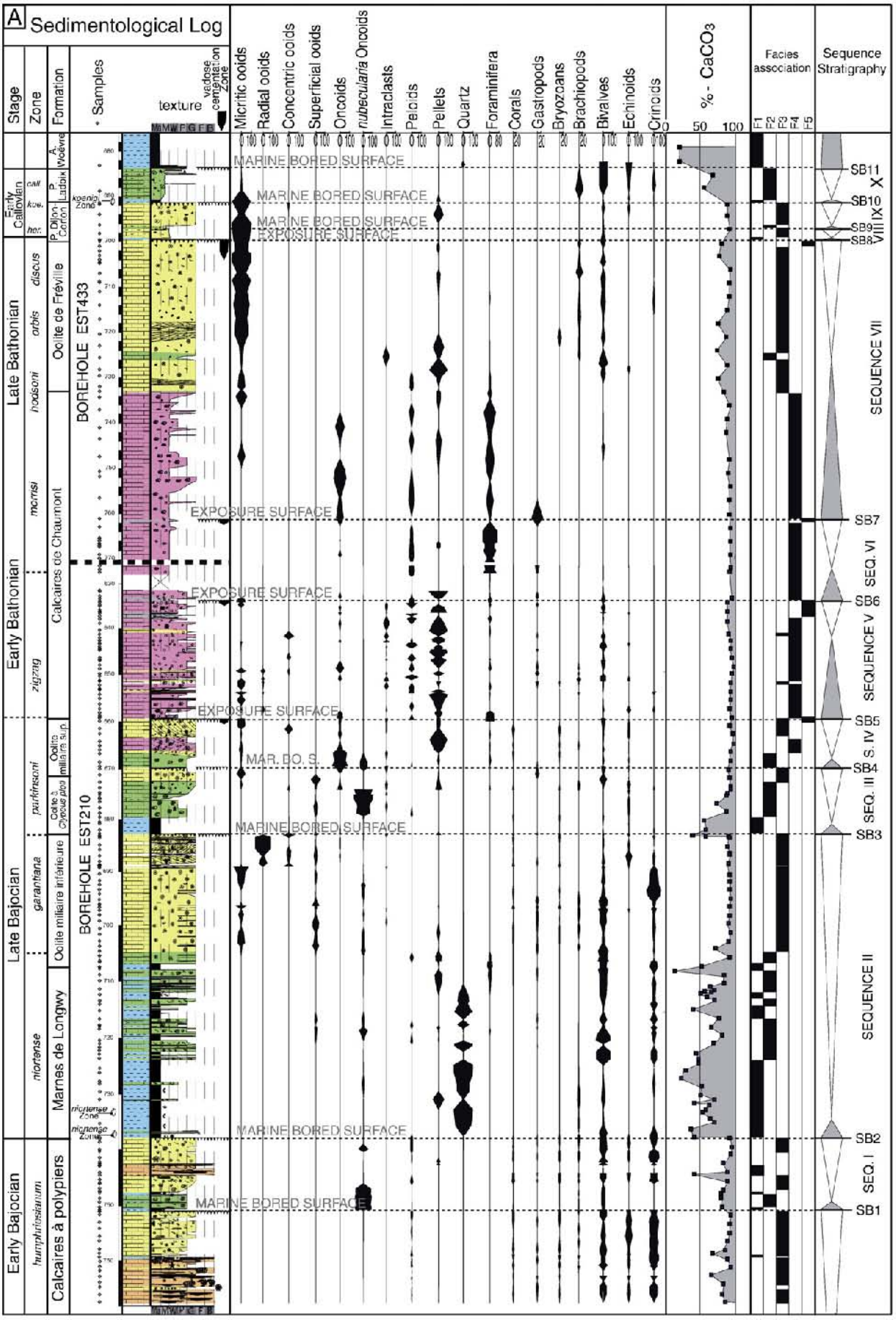
A
Sedimentological Log
Stage
Zone
Formation
Samples
texture
vadose cementation Zone
BOREHOLE EST433
BOREHOLE EST210
Micritic ooids
Radial ooids
Concentric ooids
Superficial ooids
Oncoids
rubeculiaria Oncoids
Intraclasts
Peloids
Pellets
Quartz
Foraminifera
Corals
Gastropods
Bryozoans
Brachiopods
Bivalves
Echinoids
Crinoids
% - CaCO3
Facies association
Sequence Stratigraphy
MARINE BORED SURFACE
EXPOSURE SURFACE
MAR. BO. S.
SB1
SB2
SB3
SB4
SB5
SB6
SB7
SB8
SB9
SB10
SB11
SEQUENCE II
SEQ. I
SEQ. III
S. IV
SEQUENCE V
SEQ. VI
SEQUENCE VII
VIII
IX
X

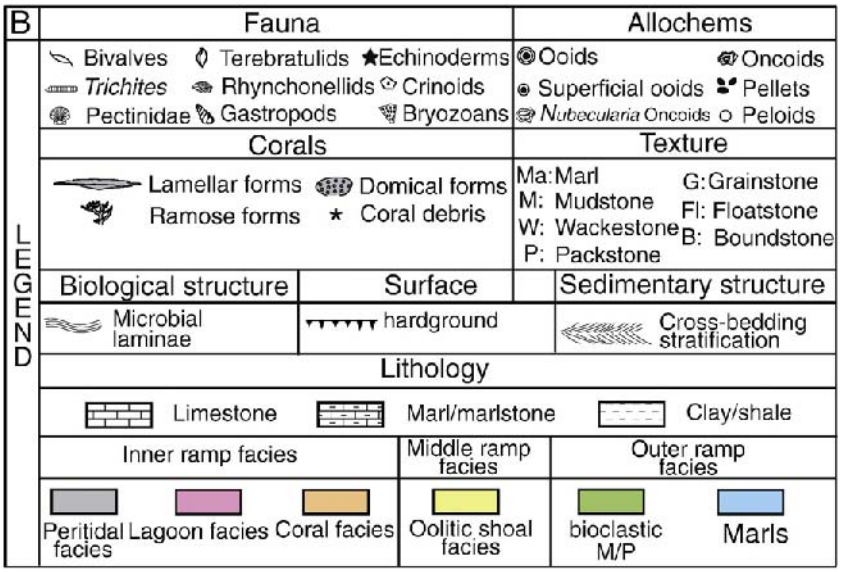

Fig. 3. A—Sedimentological log, vadose cementation, clast proportions, $CaCO_3$ percentages, facies associations and sequence stratigraphy (3rd order sequences) of the Middle Jurassic. This sedimentological log is a composite section of EST433 and EST210 Andra boreholes. B—Sedimentological log legends.

a $\delta^{18}O$ value of −2.20‰ to NBS19. Reproducibility was checked by replicate analysis of laboratory standards and was ±0.05‰ (1σ) for oxygen isotopes and ±0.02‰ (1σ) for carbon isotopes.

3.3. Carbonate production estimation

Relative carbonate production was calculated at three points along the outcropping SW–NE transect (Fig. 1): Chaumont, Neufchâteau and Nancy. Carbonate content is measured on cuttings with a GEO-RS calcimeter during the EST210 and EST433 cores drilling with a 2 m sampling step. The thickness of carbonate formations (limestones, marls and clays) and carbonate content inferred from the $CaCO_3$ content of a representative section (EST210 and EST433) was measured and accumulation rates were estimated (the carbonate thickness is divided by the corresponding biozonation duration, m/My). The siliciclastic sedimentation rate was also estimated, dividing the siliciclastic thickness by the corresponding biozonation duration (m/My). The compaction rate is not taken into account.

3.4. Clay mineralogy

Clay mineral assemblages were identified using X-ray diffraction (XRD) on 32 samples from EST210, HTM102 cores, and from outcrops (Luzy-sur-Marne, Sommerecourt, Jonchery, Neufchâteau and Champ-la-noir; Fig. 1). Samples were decarbonated, and the clay fraction (<2 µm) was separated by sedimentation and centrifugation using the analytical procedure of Holtzapffel (1985). X-ray diffractograms were obtained using a Bruker D4 Endeavour diffractometer with CuK_α radiation and a Ni filter. Semi-quantitative estimations were based on peak area summed to 100%, the relative error being 5% (Moore and Reynolds, 1989). The compilation of published clay mineral data from the Middle Jurassic interval from the Paris Basin allowed us to better constrain the mineralogical signal. Eight outcrop sections that are biostratigraphically well-constrained and with mineralogical analyses were added to the database (Sombernon, Beaume-les-Créancey, Echannay, Val Suzon, Chassagne-Montrachet, Dijon, Buffon and Chaumont, Moral, 1979; Floquet et al., 1991; Javaux, 1992).

4. Results

4.1. Sedimentary facies

Based on 18 lithofacies merged into 5 facies associations (Table 1), a composite sedimentological log of the Middle Jurassic (Bajocian to Callovian) from Andra cores (EST433 and EST210) is proposed to characterize the synthetic stratigraphic succession (Fig. 3). Observations are summarized in Table 1 and environmental interpretations are given below. The progressive lithological changes observed from a great distance along the transect (more than 100 km, Fig. 4) during the Middle Jurassic suggest a very low dipping slope without shelf breaks and gravity deposits, thus characterizing a carbonate ramp profile (Pierre et al., in press). In this paper, the ramp terminology was adopted from Burchette and Wright (1992) who define (1) an outer ramp below the storm wave base (SWB); (2) a mid-ramp between the SWB and the fair-weather wave base (FWWB), and (3) an inner ramp located above the FWWB including either high energy environments (shoreface and beach) and back-shoal infratidal to supratidal environments (e.g. muddy lagoon, tidal flats, swamps).

4.1.1. Outer ramp

In the marly facies F1, the presence of ammonites, belemnites, brachiopods and the abundant bioturbation indicates an open and distal environment. The absence of hydrodynamic structures suggests a permanent low-energy environment probably located below the SWB. The London-Brabant landmass, located 150 km to the north, may have been the source of the detrital quartz, locally abundant in this facies (Ferry et al., 2007). The water depth in this lower offshore was probably greater than 50 m.

4.1.2. Mid-ramp

Facies association F2 corresponds to marl–limestone alternations with mudstone to packstone textures. Bioturbation and abundant benthic fauna (bivalves, brachiopods, echinoids, crinoids) indicate normal oxygenation and salinities. The occurrence of hummocky cross stratification and gutter casts, suggests a sedimentation between the SWB and the FWWB. The occasional presence of hermatypic corals in biostromes, mainly composed of lamellar forms *Isastrea,* argues for an environment in the photic zone, with a water depth probably lower

than 50 m (Geister and Lathuilière, 1991; Leinfelder et al., 2002; Lathuilière et al., 2005). On the basis of the dominant allochems, facies association F2 includes (1) an oncoid packstone to wackestone (facies F2a), (2) a bivalve/echinoderm packstone to wackestone (F2b) and (3) an ooid/crinoid packstone to wackestone.

4.1.3. Inner ramp

4.1.3.1. Shoal. Facies association F3 comprises 8 lithofacies: (1) radial ooid grainstone (F3a), (2) concentric ooid grainstone (F3b), (3) micritic ooid grainstone (F3c), (4) superficial ooid grainstone (F3d), (5) bioclastics-ooid grainstone (F3e), (6) bioclastic/peloidal grainstone (F3f), (7) coral bioconstruction (boundstone texture, F3g) and (8) crinoid grainstone (F3h). In facies association F3, the presence of echinoderms, brachiopods and bryozoans in different proportions according to lithofacies suggests well-oxygenated water with normal salinity. Common cross bedding (Fig. 5E) and grainstone textures indicate a shallow environment (shoreface) corresponding to an oolitic or bioclastic shoal under tide- and wave-dominated conditions (Loreau, 1982; Javaux, 1992). The reefs, mainly observed during the Early Bajocian, belong to patch reef type (Geister and Lathuilière, 1991). The coral patch reefs recognized in this study (Fig. 5F–G), are composed of lens-shaped bodies and dome-shaped bioherms build-ups reaching 10 m thick and 10–20 m lateral extent. Predominantly lamellar forms, *Isastrea* sp., with additional taxa *Kobyastraea*, *Periseris*, and rare branching forms, these scleractinian corals constitute the main component of reefs (Geister and Lathuilière, 1991; Lathuilière, 2000b; Lathuilière, 2000a). Relief can be locally created and lateral progradation sets of facies F3f are observed (Fig. 5F–G). Coral biostromes (1–3 m large and <0.5 m thick) are also observed during the Early Callovian (Rimaucourt). In F3 facies association, common cross bedding, grainstone texture and coral bioconstructions probably developing under oligotrophic conditions, argue for a depositional environment above the FWWB (Geister and Lathuilière, 1991; Leinfelder et al., 2002). The water depth in this high energy environment is probably lower than 30 m.

4.1.3.2. Lagoon. Three facies are distinguished in facies association F4: (1) peloidal/foraminiferal mudstone/packstone (F4a), (2) oncoids–peloids grainstone/packstone (F4b) and (3) pellets grainstone/packstone (F4c). In F4a and F4b (Fig. 6E), the abundance of lime mud indicates low hydrodynamic conditions. The size distribution of allochems and the diversity of components in facies F4a including oncoids, peloids, ooids, miliolids, bivalves, intraclasts, *Cayeuxia* and *Ortonella* cyanobacteria suggest possible periodic re-sedimentation by storm currents. Oncoids and very well-preserved gastropods are often interpreted as having been deposited in protected lagoonal environments. Pellet facies associated with Miliolina foraminifera, oncoids, ooids and *Cayeuxia* cyanobacteria is also common in lagoon environments (Fig. 6F).

4.1.3.3. Intertidal to supratidal environments. Laminated micritic deposits with fenestrae, mud cracks and root traces are common in the Bathonian facies under study, suggesting intertidal environments. The presence of carbonate wash-over deposits forming flat islands is also well documented within the Bathonian carbonate deposits (Purser, 1975; Javaux, 1992). These islands were surrounded by coarse calcarenitic beaches mainly composed of micritic intraclasts, oncoids and large bioclasts (Fig. 6G). Meniscus and pendent cements are commonly observed in these beach deposits (Fig. 6G). They indicate that beachrocks contributed to the nucleation, expansion and preservation of the wash-over islands. In supratidal flat islands, in very low energy environments, brackish or brine ponds with charophytes and type-III organic matter decantation may have given rise to lignite layers (F5c facies). The lithofacies association F5 marks very proximal environments on the foreshore.

4.2. Biosedimentary system changes in the sequence stratigraphic framework

Following the sequence definition of Vail et al. (1977) re-examined by Jacquin et al. (1998) for Mesozoic series of European basins, 10 depositional sequences (Sequences I to X; Fig. 4) were recognized from the Early Bajocian (*humphresianum* Zone) to Early Callovian (*koenigi* Zone), on the basis of vertical facies succession and bounding surfaces (Sequence Boundaries SB1 to SB11) along the study transect (Fig. 4). The boundary between sequences is generally marked by an abrupt vertical facies change from shallow to deep (flooding surface). This deepening is usually underlined by a flat bored surface due to the conjugate action of marine cementation, mechanical abrasion and marine boring organisms (bivalves, annelids and echinoids). Demonstrable evidence of terrestrial exposures (vadose cements, phreatic meteoric cements, pedogenesis or karstification) extending all along the inner ramp settings is only observed in association with SB5, SB6, SB7 and SB8 bounding surfaces, that require a relative sea level fall. Due to the relative proximal deposition of the carbonate system and the probably low amplitude of eustatic variations, Lowstand System Tracts (LST) are only observed in Sequences V, VI and VII during sea level drop inferred from exposure surfaces (SB6, SB7 and SB8). These sequences are previously recognized in the Paris Basin as third-order cycles (Garcia et al., 1996a; Gaumet et al., 1996; Hardenbol et al., 1998; Jacquin and de Graciansky, 1998). At a longer time scale, the 10 third-order sequences are stacked into 4 biosedimentary packages (Figs. 4 and 7), which are distinguished on the basis of allochem assemblages and sedimentary architectures.

4.2.1. Early Bajocian–Crinoidal accumulations and coral reef development (Sequence I)

The Early Bajocian limestones (*Calcaires à polypiers*) are mainly characterized by bioclastic facies (crinoid- and bivalve-rich packstone and grainstone; facies F3f and F3h, Fig. 6B–C), coral-rich facies (F3g) and *Nubecularia* oncoid wackestone/packstone facies (F2a; Figs. 5 and 6A). Echinoderms, bryozoans, bivalves, brachiopods, and coral debris form the main allochems of this period. Some coral reefs induced palaeoslopes up to 10–15 m high (Figs. 4 and 7A) comparable to well-exposed reef slopes that have been described 50 to 100 km southwestward, in the Haute-Marne department and Burgundy (Durlet et al., 2001b). The carbonate system can be represented as a long-scale intra-cratonic carbonate ramp with an extensive coral reef development in the eastern part of the Paris Basin (Geister and Lathuilière, 1991; Lathuilière, 2000a,b; Leinfelder et al., 2002).

In the study area, the Early Bajocian limestones are about 30 m thick. The lowermost part of these deposits is dated to the *laeviuscula* Zone (*Calcaires d'Ottange*; Fig. 2) and *propinquans* Zone (*Calcaires de Haut-Pont*; Fig. 2), which are only observed in the north-eastern part of the transect by Guillocheau et al. (2002). A large part of the transect is represented only by deposits (*Calcaires à polypiers*) dated to the *humphresianum* Zone by ammonites and brachiopods (Thierry et al., 1980; Mangold et al., 1994). These carbonate deposits are subdivided into three Members (*Calcaires à polypiers inférieurs*, *Oncolite Cannabine* and *Calcaires à polypiers supérieurs*). The *Oncolite Cannabine* and *Calcaires à polypiers supérieurs* deposits form a 20 m-thick aggrading–prograding sequence documented by Guillocheau et al. (2002) in the study area. This sequence (Sequence I) is dated to the *blagdeni* Sub-Zone (Mangold et al., 1994). Its lower surface marked an abrupt facies change from bioclastic grainstone (F3 facies association) in the *Calcaires à polypiers inférieurs* to oncoid wackestone/marl alternations (F2 facies association) in the *Oncolite cannabine*. This boundary is a bored surface, grains are early cemented by Isopachous Fibrous Calcite (IFC) cements. These cements are truncated by borings and commonly overlapped by geotropic micritic internal sediments. They are inclusion-rich and exhibit a cloudy

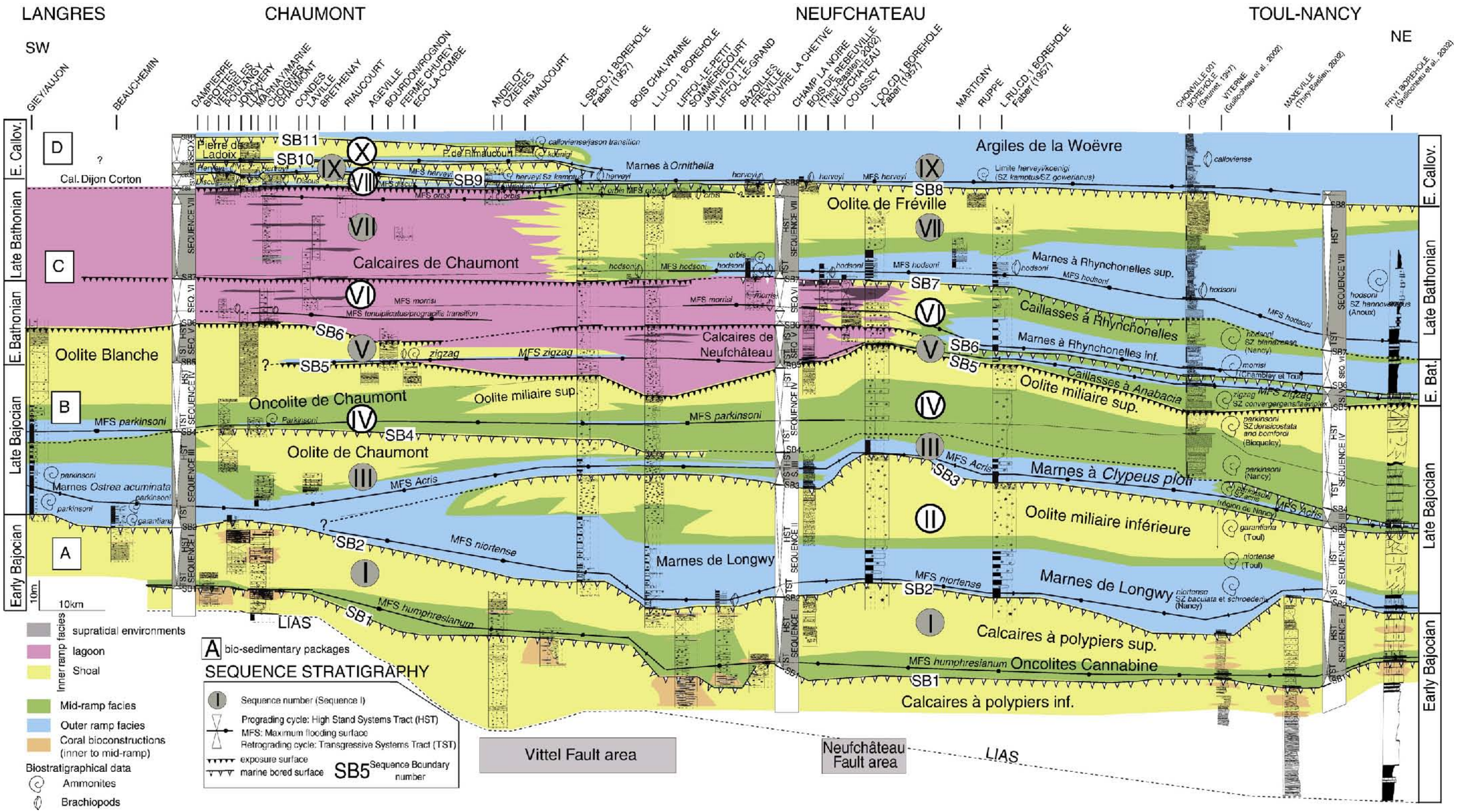

Fig. 4. Correlation diagram of the Middle Jurassic in the eastern Paris Basin on a Langres–Nancy transect. This illustration is composed of the 37 outcrop sections and one core studied in this work completed by previous descriptions of five cores (Faber, 1957; Gaumet, 1997; Guillocheau et al., 2002) and three outcrop sections (Guillocheau et al., 2002). Correlations are based on well dated flooding surfaces by biostratigraphy (ammonite and brachiopod associations) and 10 recognized sequence stratigraphic cycles (I to X) delimited by Sequence Boundaries (SB1 to SB11).

brown-to-yellow luminescence. Such characteristics of IFCs probably indicate their initial HMC (High Magnesium Calcite) mineralogy, precipitating from phreatic marine waters (Brigaud et al., in press).

The upper surface is a major discontinuity at the Paris Basin scale (e.g. Durlet et al., 2001b; Vesulian unconformity: SB2; Fig. 5D) marked by a bored surface with submarine cementation, submarine bioerosion and a drastic facies change from bioclastic grainstone (F3f) to oyster coquina beds and marls (F1). In the study area, clear exposure evidence is not observed below SB2.

4.2.2. Late Bajocian—Ooid ramp development (Sequences II, III and IV)

The Late Bajocian limestones (*Oolite miliaire*) are mainly composed of ooid grainstone facies (F3a–d, Figs. 5 and 6A). The transect (Figs. 4 and 7B) displays a general south-west dipping ramp, with a proximal area in the north-eastern part built alongside the London-Brabant Massif in the Ardennes (*Oolite de Doncourt*; Thierry et al., 1980) and the distal part near the south-western part of the study area where marly deposits (F1; *Marnes à Ostrea acuminata*) replace the ooid facies (F3a–d; *Oolite miliaire*). Along the transect (Figs. 4 and 7B), the depositional system evolves from inner ramp (F3a–e) to outer ramp (F2a, F2b and F1 facies). Three third-order sequences, with aggrading to prograding geometries, are recognized in these deposits (Sequences II, III and IV). SB2, SB3 and SB4 are bored surfaces which are cemented by 20–50 µm thick marine IFC cements, initially in HMC mineralogy. No meteoric diagenetic phases (cements, pedogenesis or dissolution features) are associated with these surfaces. The HSTs, which show shallowing-up vertical evolution from F1 to F3 facies associations, reveal well-expressed aggrading–prograding ooid wedges that mainly prograde south-westward (Fig. 4; *Oolite miliaire inférieure*, *Oolite de Chaumont* and *Oolite miliaire supérieure*). The three TSTs are successively marked by the *Marnes de Longwy*, *Oolite à Clypeus ploti* and the *Marnes à Ostrea acuminata* (Fig. 4). Ammonites allow us to date the MFS (maximum flooding surface) of Sequence II to the *niortense* Zone in *Marnes de Longwy*, the MFS of Sequence III to the *parkinsoni* Zone (acris Sub-zone) in *Oolite à Clypeus ploti* and *Marnes à Ostrea acuminata*, and the MFS of Sequence IV to *parkinsoni* Zone in *Marnes à Ostrea acuminata* (Mangold et al., 1994). At the end of Sequence IV, ooid deposits covered the entire study area.

4.2.3. Bathonian—Muddy ramp (Sequences V, VI, and VII)

The Bathonian carbonate formations are mainly composed of micritic facies (facies association F4, *Calcaires de Chaumont*, Figs. 4 and 7C) and ooid grainstones (F3a–d; *Oolite Blanche* and *Oolite de Fréville*). The transect (Figs. 4 and 7C) displays a new ramp orientation, now dipping to the north–east with a proximal area in the south (lagoonal facies F4 of the *Calcaires de Chaumont*) and a distal part to the north–east (marl facies F1; *Marnes à Rhynchonelles*).

The Bathonian period is marked by the development of a large protected inner ramp environment (lagoonal, intertidal and supratidal facies, Figs. 1, 4 and 7C). In the study area, depositional environments evolve laterally from supratidal facies associations (F5), through lagoonal (F4) and shoal inner-ramp facies (F3a–e), to mid and outer ramp facies (F2a, F2b and F1 facies). Three stratigraphic sequences can be recognized (Sequences V, VI and VII, Fig. 4) separated by two bored surfaces (SB6 and SB7; Fig. 5C).

The lower surface of Sequence V (SB5) is locally cemented by microstalactitic cements that developed up to a few centimetres down from the surface in core EST210. These pendent cements are characterized by inclusion-poor crystals of non-ferroan calcite, which are non-luminescent with few brightly luminescent growth bands. Such characteristics indicate a vadose environment, an initial LMC mineralogy and suggest a meteoric or mixed parent waters which probably percolated downward during a sea level drop.

SB6 characteristics evolve from the south–west to the north–east (basinward). At the south–west, near Chaumont, it is an exposure surface with karstic features and root traces at the top of the *Oolite Blanche* (Purser, 1989). SB6 is frequently covered by a lignite layer or early cemented by microstalactitic cements (EST210 core), indicating an exposure episode (Floquet et al., 1991). At the north–east, at the top of the *Caillasse à Anabacia,* SB6 is a single flat bored surface with only marine IFC cements, covered by marls (*Marnes à Rhynchonelles inférieures*). This allows us to interpreted the top of the *Caillasse à Anabacia* as a possible LST during a sea level drop (Fig. 4).

SB7 (Fig. 5C) usually corresponds to a marine flat bored surface with IFC marine cements truncated by bivalves and annelids borings. However, SB7 evolves to an irregular discontinuity overlying coarse grainstone to rudstone deposits, and truncating non-luminescent microstalactitic calcitic cements (EST433 core, F5b, Fig. 6G). As for SB5 and SB6, theses cements suggest an exposure episode probably coeval with LST deposits (*Cailasse à Rhynchonelles,* Fig. 4). Sequence VII is marked at the base by a thick TST with marl deposits to the north–east, which can drown the lagoon as recognized in the Neufchâteau outcrop during the *hodsoni* Zone (*Marnes à Rhynchonelles supérieures*; Fig. 4). The same event is also recorded in southern Burgundy with a marl invasion (*Marnes à Pholadomya*; Garcia et al., 1996a, Gaumet et al., 1996) over proximal carbonate deposits and is well-detected in the Boulonnais area (North of France, Vidier et al., 1995) in the *hodsoni* Zone. Aggradation of lagoonal facies (*Calcaires de Chaumont*; Sequence VII; facies F4) and the progradational trend of the ooid facies define the HST of this sequence (*Oolite de Fréville*; Sequence VII; facies F3a–d, Fig. 8A–B). Its top is marked by SB8 (D1 *sensu* Floquet et al., 1989; Fig. 5A–B), which is also recognized in Burgundy and Lorraine (Floquet et al., 1989, 1991; Javaux, 1992; Mangold et al., 1994). Non-luminescent meniscus LMC cements developed below SB8 (Fig. 6F), through the upper 4 m of the *Oolite de Fréville* in EST433 core (Figs. 3A and 7C). Below this 4 m-thick of meniscus cement developments, non-luminescent scalenohedral and blocky early spar cements developed contemporaneously to the meniscus cements in core EST433. Such characteristics indicate a meteoric phreatic zone developed below a meteoric vadose zone during an exposure event. The vertical development of meteoric vadose cements below SB8 suggests a sea-level fall of at least 4 m. In protected lagoon environments near Chaumont, SB8 exposure surface is marked by an irregular surface with root traces (paleokarst; Fig. 5B). Exposure surface SB8 probably corresponds to a LST with ooid shoal progradations (*Oolite de Fréville*) in the north-eastern transect during this sea level fall (Fig. 8C). Upper surface SB8 of this LST is a submarine surface with IFC cement development near Neufchâteau, during a drowning event (Fig. 8D).

4.2.4. Uppermost Late Bathonian–Early Callovian—Oobioclastic ramp development (Sequences VIII, IX and X)

The Early Callovian formations (Dijon-Corton Limestone and Ladoix Limestone) are mainly composed of oobioclastic grainstones (facies association F3, Figs. 4 and 7D) that are sometimes rich in brachiopods, bryozoans, coral debris and crinoids (e.g. the *Pierre de Rimaucourt* in Fig. 2 and 4). Lagoon environments disappear in the study area at the end of Bathonian (Javaux, 1992; Garcia et al., 1996a; Gaumet et al., 1996; Gaumet et al., 2001). In northern Burgundy, well-preserved conifer needles (*Brachyphyllum, Palaeocyparis*), filicoides forms (*Lamatopteris* genus) and cycadophytes (*Otozamites, Sphenozamites*) have been found in the *Calcaires à Plantes* of the Etrochey quarry, indicating nearest islands (Lemoigne and Thierry, 1968; Gaumet et al., 1996). Consequently, the ramp morphology evolved from localized islands and ooid shoals in the south–west (Burgundy to Chaumont; F3) to a marly outer ramp in north–east (Neufchâteau to Nancy; F1, F2; *Argiles de la Woëvre*; Fig. 7).

The uppermost Late Bathonian–Early Callovian limestones are subdivided into 3 third-order sequences (Sequences VIII, IX and X) separated by marine bored surfaces (SB9 and SB10), with only marine cements truncated by borings. Above SB8, the *Marnes à Eudesia*,

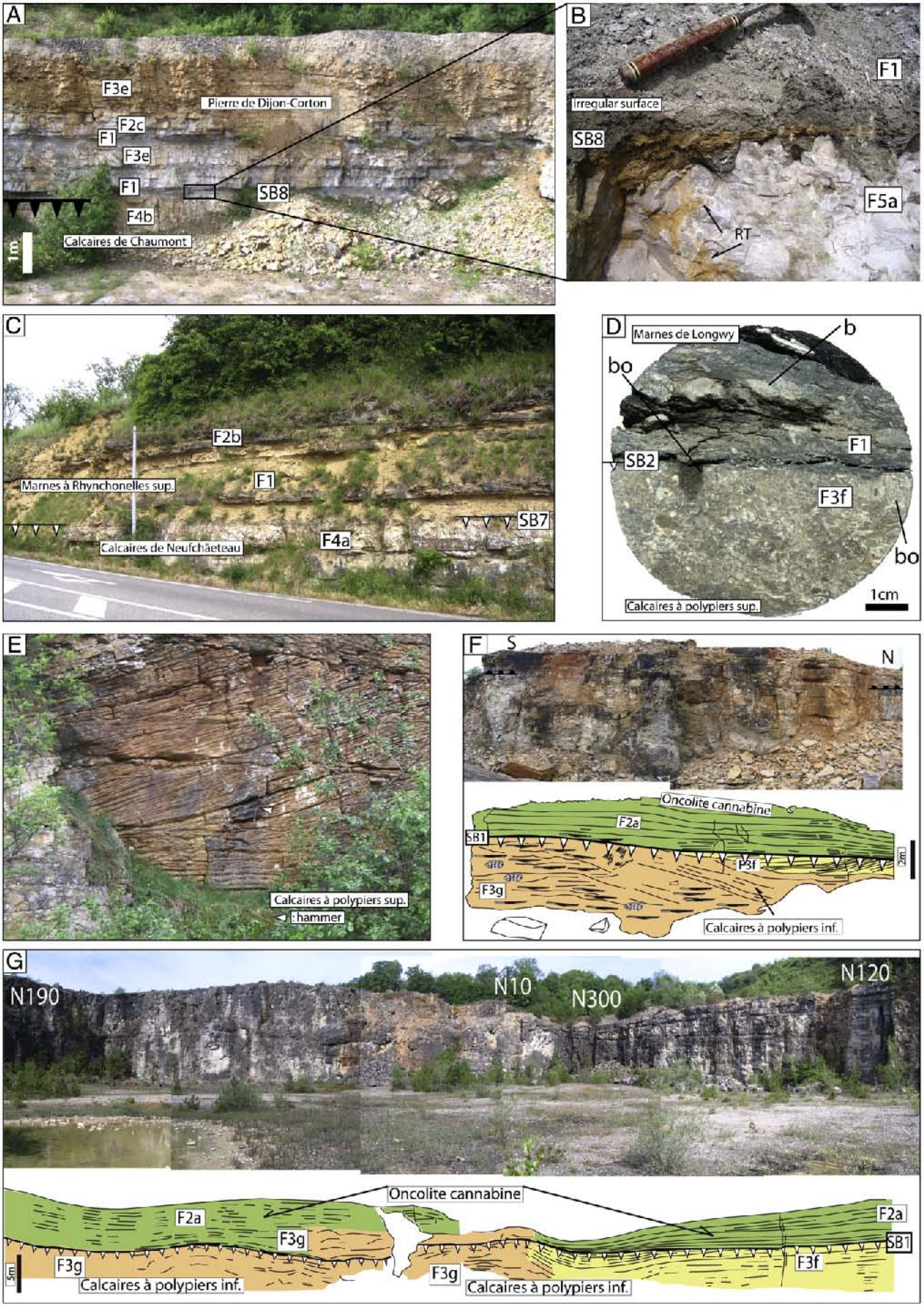
A
F3e
Pierre de Dijon-Corton
F2c
F1
F3e
F1
SB8
F4b
Calcaires de Chaumont
1m
B
F1
Irregular surface
SB8
F5a
RT
C
F2b
F1
Marnes à Rhynchonelles sup.
SB7
F4a
Calcaires de Neufchâteau
D
Marnes de Longwy
b
bo
F1
SB2
F3f
bo
Calcaires à polypiers sup.
1cm
E
Calcaires à polypiers sup.
hammer
F
S
N
Oncolite cannabine
F2a
SB1
F3f
F3g
2m
Calcaires à polypiers inf.
G
N190
N10
N300
N120
Oncolite cannabine
F2a
F3g
F2a
SB1
F3g
F3f
5m
Calcaires à polypiers inf.
F3g
Calcaires à polypiers inf.

Marnes à Ornithella and *Argiles de la Woëvre* deposits form the TST of the Sequence VIII (Fig. 8D). MFS, dated by brachiopods of the *discus* Zone, occurs in these marls levels. The following HST is marked by shallowing-up with progradations of bioclastic and ooid bodies (Fig. 8E). The shallow F3e facies is only located in the south-western part of the transect (Fig. 4). It developed within a retrogradational sequence with a decline of the previous well-developed carbonate system. The geometries in Fig. 4 illustrate the retrogradational trend in the study area at the Bathonian/Callovian transition. The TST of Sequence IX flooded the previous carbonate deposits of Sequence VIII (Fig. 4). This sequence is dated by brachiopods and ammonites to the *herveyi* Zones which marked its MFS, as in Chaumont, Jonchery or Andelot outcrops (Fig. 4); (Floquet et al., 1989, 1991). Limited ooid progradation (*Pierre de Dijon-Corton*) on the ramp is observed in the south-western part of the study transect (HST, Sequence IX; Fig. 4). Sequence X corresponds to a TST with marl deposits, followed by a HST (*Pierre de Ladoix, Pierre de Rimaucourt)*. Brachiopods and ammonites date this sequence to the *calloviense* Zone (Courville and Raffray, 2007). The top surface SB11 of Sequence X is a major discontinuity in Burgundy (D3 *sensu* Floquet et al., 1989) marked by a drastic facies change from crinoid-rich oobioclastic grainstones to iron-ooid bearing marls. This discontinuity without any evidence of subaerial exposure is bored by polychets and bivalves under marine conditions as earlier suggested by Purser (1969).

4.2.5. Middle and Late Callovian—Marly outer ramp

The Middle and Late Callovian is characterized by thick clay deposits (150 m) with a rich ammonite fauna indicating an outer ramp environment. It corresponds to a period of carbonate depletion, replaced by siliciclastic marly and clayey sedimentation (Collin et al., 1999, 2005; Collin and Courville, 2006; Thierry et al., 2006).

4.3. Oxygen isotopes

The 197 oxygen isotopic values of the 94 LMC shells and rostra range from −2.9 to 0.6‰ PDB in $\delta^{18}O$ (Fig. 9C and Appendix A). The values show a quite large variability either between shells from the same bed or within a single oyster shell. The intra-shell variability has been quantified using the difference between maximum and minimum $\delta^{18}O$ values of bivalves that have more than 2 isotope analyses. The mean value of intra-shell variability for all analysed *Trichites* and oysters is 0.5‰, and reaches a maximum of 1.6‰ in a sample. The *Trichites* and oyster shells recovered in a same stratigraphic bed display similar values, as seen in the Rimaucourt outcrop ($\delta^{18}O$ mean value of −1.9‰ PDB for *Trichites* and −1.8‰ PDB for oysters; Appendix A) or from the Pouillenay quarry ($\delta^{18}O$ mean value of −0.8‰ PDB for a *Trichites* and −0.7‰ PDB for an oyster; Appendix A). The $\delta^{18}O$ values of *Trichites* or oyster shells are slightly lower (0.5–0,7 ‰) than the values of belemnite rostra collected from a same bed in the Pouillenay outcrop (uppermost *Calcaires à polypiers*; level 31.2 m and uppermost *Marnes à Ostrea acuminata*, level 41 m Appendix A). The $\delta^{18}O$ values of bivalves are the same for different environments during a given stratigraphic interval. For example, during the *garantiana* Zone or *parkinsoni* Zone , $\delta^{18}O$ values for oysters from the outer ramp (−0.5 to −1.5‰ PDB; *Marnes à Ostrea acuminata*; Fig. 9C) are similar to values for ooid shoals of inner ramp (−0.5 to 1.5‰ PDB; Oolite miliaire; Fig. 9C).

Despite the variability displayed in oxygen isotope values, $\delta^{18}O$ values of non-luminescent oyster shells exhibit variations along the studied stratigraphic interval (Fig. 9C). During the *humphresianum* Zone, $\delta^{18}O$ values vary between −2.9‰ PDB and −0.5‰ PDB with an average of −1.5‰ PDB calculated on 100 $\delta^{18}O$ values measured on 34 *Trichites* shells and one oyster shell. From the Early Bajocian (*humphresianum* Zone) to the Late Bajocian (*garantiana and parkinsoni* Zones), $\delta^{18}O$ increases to average values of −1‰ PDB with values between −1.9 and −0.3‰ PDB (Fig. 9C). During the *hodsoni* Zone, only one non-recrystallized *Trichites* has been found, and only three values were measured; they reveal $\delta^{18}O$ of −1‰ PDB on average which is similar to values measured in the Late Bajocian and the Earliest Callovian. In the *discus* and *herveyi* Zones, 16 $\delta^{18}O$ values of seven oyster shells (*Ostrea* sp.) range from −1.9‰ PDB to 0.6‰ PDB with a mean value of −0.6‰ PDB. $\delta^{18}O$ values of *Trichites* and oyster shells from the *calloviense* Zone are about 1.2‰ PDB lower, with average values of −1.8‰ PDB (Fig. 9C). One oyster shell from the *jason* Zone of the Middle Callovian yields three values comparable to that found for the *calloviense* Zone, ranging from −2‰ PDB to −1.4‰ PDB with a mean value of −1.7‰ PDB.

4.4. Carbon isotopes

The 197 new carbon isotopic compositions of the 94 LMC shells and rostra range from −0.8‰ PDB to 4.4‰ PDB in $\delta^{13}C$ (Fig. 9E and Appendix A). These new data are included in a compilation of $\delta^{13}C$ data from bivalves and belemnites sampled from England (Anderson and Arthur, 1983; Podlaha et al., 1998; Jenkyns et al., 2002; Price and Page, 2008), Scotland (Jenkyns et al., 2002), Portugal (Jenkyns et al., 2002), Bulgaria (Metodiev and Koleva-Rekalova, 2008), Poland (Wierzbowski and Joachimski, 2007), Germany (Podlaha et al., 1998) and Russia (Podlaha et al., 1998; Riboulleau et al., 1998), in order to generate a compilation curve for the Tethyan domain (Fig. 9E). A composite curve from bulk analysis of the pelagic domain (Umbria Basin, Italy; Subbetic Basin, Spain; South-East Basin, France) is also reported in Fig. 9E (Corbin, 1994; Bartolini et al., 1999; Bartolini and Cecca, 1999; O'Dogherty et al., 2006). From the *discites* Zone to the *humphresianum* Zone, $\delta^{13}C$ values for bivalve and belemnite shells increase from 1‰ PDB to 4‰ PDB (Fig. 9E), mirroring the shift recorded in pelagic environments on bulk samples and on fossil woods from England (Hesselbo et al., 2003). A $\delta^{13}C$ decrease is observed on belemnite guards from England (Jenkyns et al., 2002) from 4‰ in the *humphresianum* Zone to 1‰ in the *parkinsoni* Zone (Fig. 9E), which is similar to that documented for bulk carbonate samples from the pelagic domain of the western Tethys Sea (Corbin, 1994; Bartolini et al., 1999; Bartolini and Cecca, 1999; O'Dogherty et al., 2006). Carbon-isotope values remain relatively stable and low during the Bathonian both for bivalve and belemnite shells and for bulk rock (Fig. 9E). An increase to average values of 3–4‰ is observed during the Callovian both in bivalves and belemnites, and bulk rock samples (Fig. 9E and Appendix A).

Fig. 5. A—Jonchery quarry displaying the *Calcaires de Chaumont* (lithofacies F4b: Oncoids–Peloids Packstone, lagoon, inner ramp) and the *Pierre de Dijon-Corton* (Marly lithofacies F1 of outer ramp, Ooids/crinoids Wackestone/Packstone lithofacies F2c of mid-ramp and oobioclastic Gainstone lithofacies F3e of inner ramp). B—Sequence Boundary-SB8 marked by an irregular (probably karstified) surface associated with root traces (RT), indicating supratidal environments (F5a lithofacies *Calcaires de Chaumont*, Jonchery quarry). C—Neufchâteau outcrop displaying the *Calcaires de Neufchâteau* (lithofacies F4a: Peloidal/foraminiferal Mudstone/Packstone, lagoon environment)/*Marnes à Rhynchonelles inférieures* (Marly lithofacies F1, outer ramp; and Bivalves/echinoderms Wackestone/Packstone lithofacies F2b, mid-ramp environments) transition—SB7. D—Bored surface SB2 (Vesulian unconformity, in EST210 core 738 m depth) separating the *Calcaires à polypiers supérieurs* (lithofacies F3f: bioclastic peloidal Grainstone, inner ramp) and the *Marnes de Longwy* (Marly lithofacies F1, outer ramp), bo: boring, b: brachiopod. E—Cross bedding stratification in bioclastic peloidal grainstone (lithofacies F3f—*Calcaires à polypiers supérieurs*; Ozières quarry, inner ramp environments). F—Domal bioherms composed of scleractinian corals with massive forms and phaceloid ramose forms (lateral extent of 30 m and 3 m thick; coral lithofacies F3g, inner ramp environments). The lateral F3f lithofacies displays cross bedding (*Calcaires à polypiers inférieurs*, Dampierre quarry). G—Coral reef (F3g facies; 15 m thick and lateral extent >50 m) and F3f lithofacies (bioclastic/peloidal Grainstone, inner ramp environments). SB1 separates coral patch-reef (*Calcaires à polypiers inférieurs*) to *Oncolite cannabine* (F2a lithofacies, mid-ramp environments); Sommerécourt quarry.

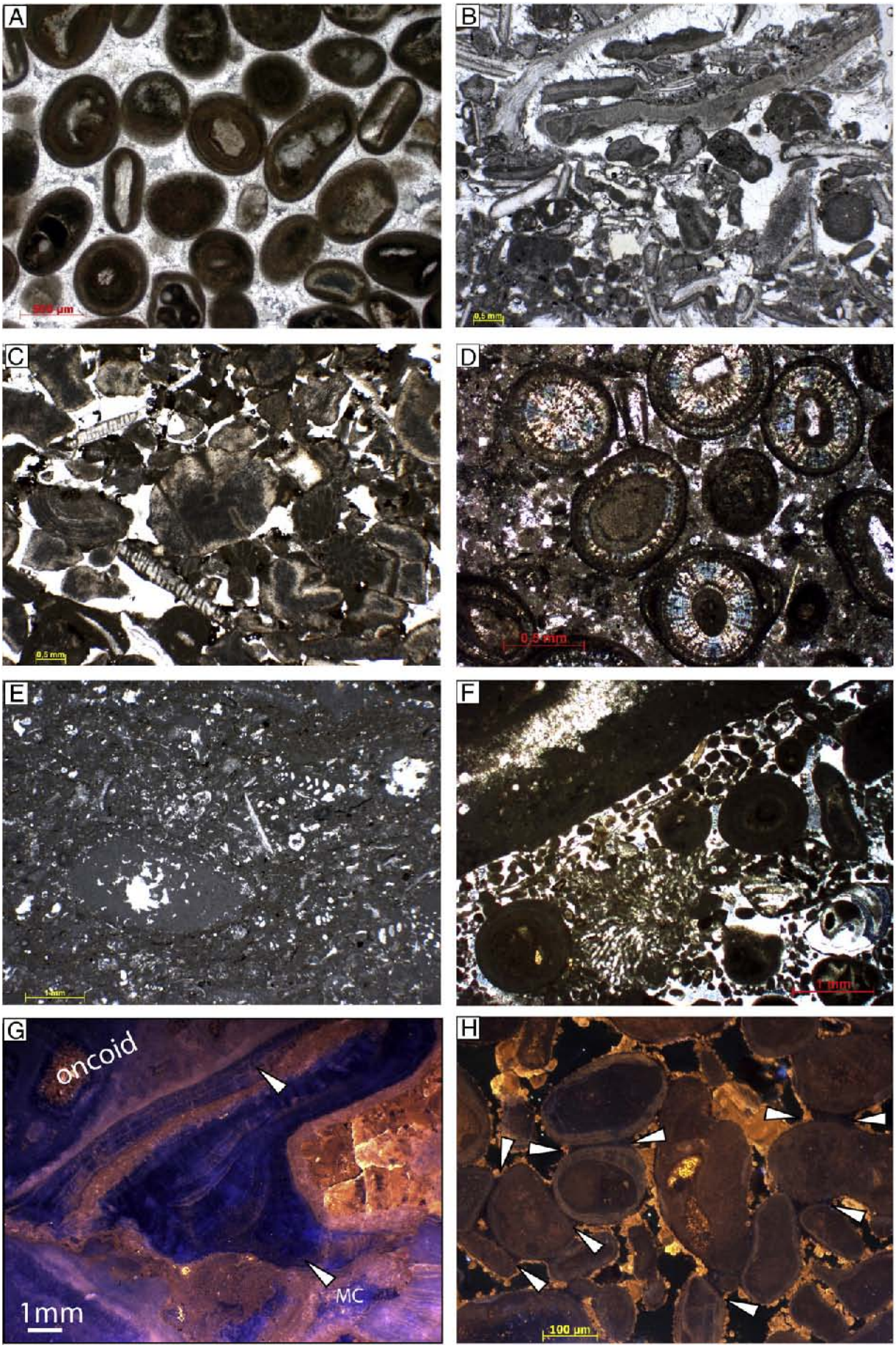
A
B
C
D
E
F
G
oncoid
MC
1mm
H
100 µm

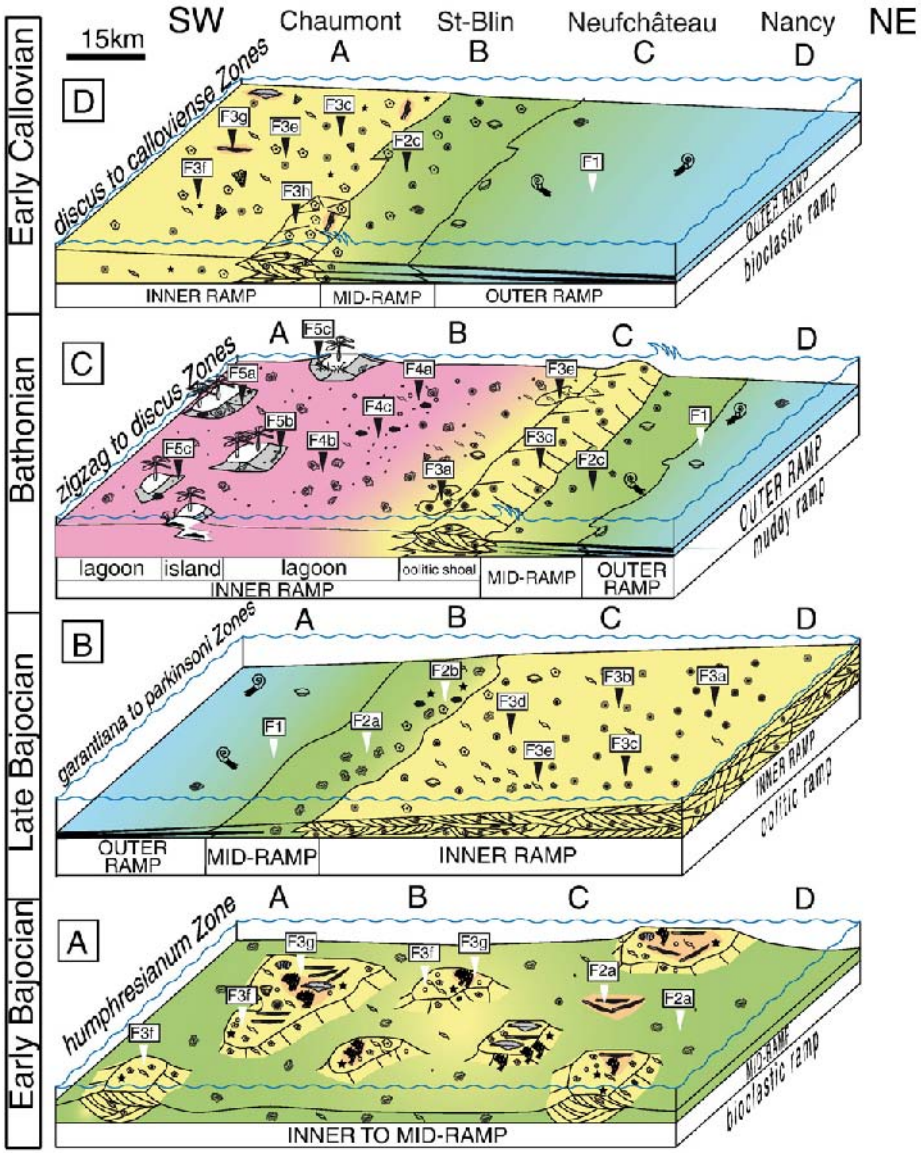

Fig. 7. Facies distribution and palaeoenvironmental reconstruction of the eastern Paris Basin during four successive steps. Lithofacies are indicated by numbers.

4.5. Carbonate production and siliciclastic sedimentation rate

Neritic carbonate production is quantified along the study transect (Fig. 9F and Appendix B). Carbonate production was maximal during the Early Bajocian (*humphresianum* Zone) where carbonate formations occurred everywhere along the transect with an average carbonate sedimentation rate of about 60 m/My (Fig. 9F). A first carbonate crisis is recorded in the *niortense* Zone with an average rate decreasing to 8 m/My, while the siliciclastic sedimentation rate increased to 30 m/My during the Early Bajocian to the Late Bajocian. Carbonate production, mainly composed of ooids, oncoids and bivalves, increased in the *garantiana* Zone and peaked in the *parkinsoni* Zone (65 m/My, Fig. 9F and Appendix B). The Early Bathonian is characterized by low carbonate productivity (15 m/My) and low siliciclastic sedimentation rates (8–17 m/My). From the *hodsoni* Zone to the *orbis* Zone, carbonate and siliciclastic sedimentation rates increased respectively to about 25 m/My and 35 m/My (Fig. 9F). Carbonate productivity then fell between the *orbis* Zone and the *discus* Zone to values of less than 5 m/My. In the eastern Paris Basin, carbonate productivity was low during the Early Callovian (4 m/My on average) and very low at the beginning of the Middle Callovian (<5 m/My) whereas siliciclastic production increased to about 35 m/My.

Fig. 6. A—Ooid grainstone characterizing shoal environments of the Late Bajocian/Bathonian interval (F3c lithofacies—*Oolite miliaire inférieure*, E078 sample, EST210 core). B—Peloidal/bioclastic grainstone with brachiopods, bivalves and echinoderms characterizing shoreface environments during the Early Bajocian (F3f lithofacies—*Calcaires à polypiers supérieurs*, E127 sample, EST210 core). C—crinoid-rich grainstone with bryozoans and brachiopods characterizing shoal environments (inner ramp) during the Early Bajocian and Early Callovian (F3h—*Pierre de Rimaucourt*, Rimaucourt). D—Radial ooid packstone characterizing protected shoal in inner ramp environments (F3b lithofacies—*Oolite miliaire inférieure*, CAR19 sample, L.LI.CD1 core). E—Peloidal/foraminiferal wackestone with oncoids and organic matter characterizing muddy lagoon environments, inner ramp (F4a—*Calcaires de Chaumont*, sample E043, EST210 core). F—Pellet/oncoid grainstone with ooids and *Cayeuxia* porostromate, characterizing lagoon and inner ramp (F4c—*Calcaires de Chaumont*, sample E040, EST210 core). G—Bioclastic and oncoid rudstone with non-luminescent meniscus and stalactitic cements characterizing beach rock environments during a sea level fall (SB7); (F5b lithofacies—*Calcaires de Chaumont*, sample E438, EST433 core). H—Non-luminescent low magnesium calcite forming Meniscus Cement (MC) between ooids and bioclasts under SB8 reflecting sea level fall and exposure period (F3c—*Oolite de Fréville*, E409 sample, EST433 core).

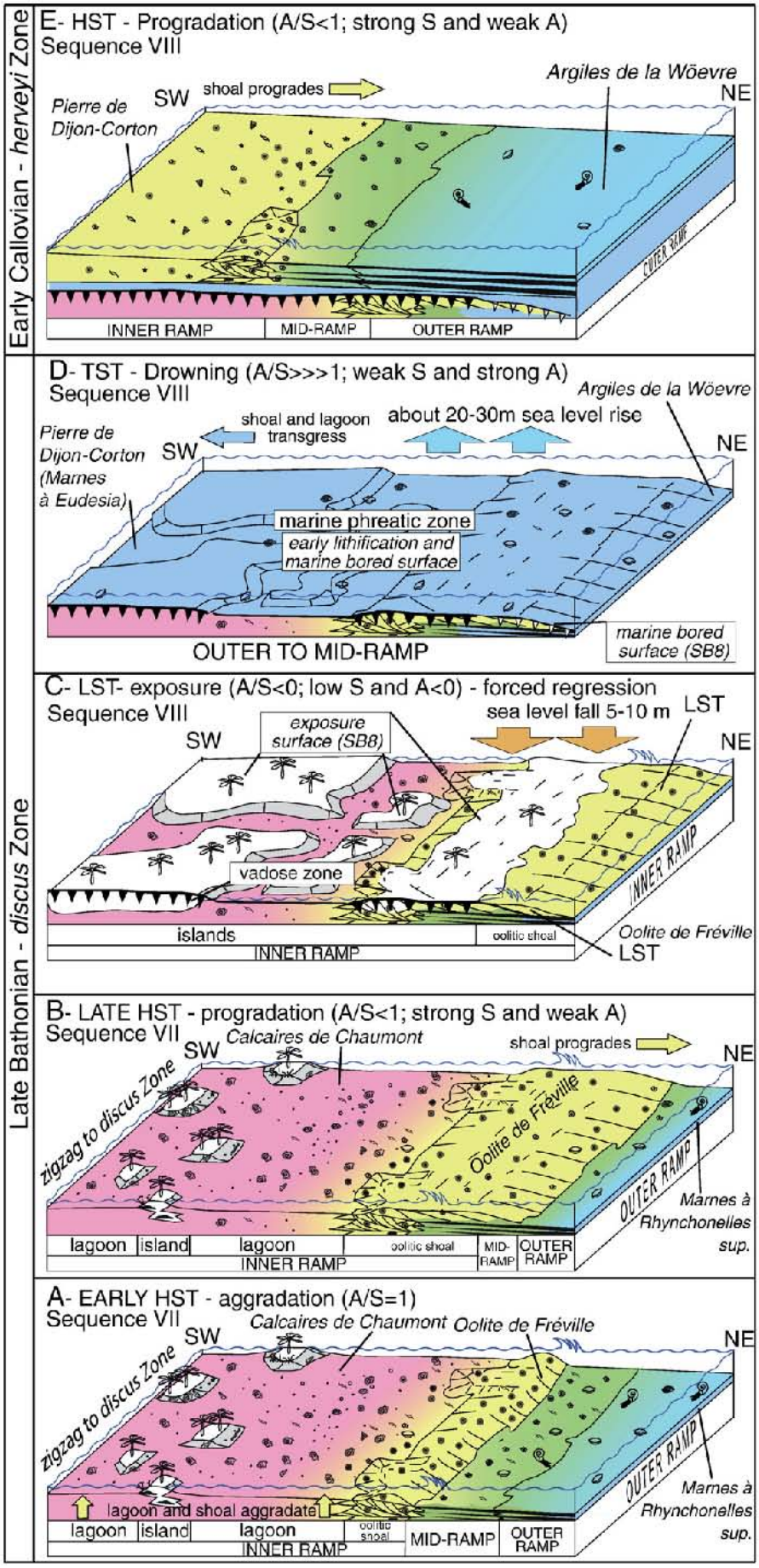
Early Callovian - herveyi Zone
Late Bathonian - discus Zone
E- HST - Progradation (A/S<1; strong S and weak A)
Sequence VIII
Argiles de la Wöevre
shoal progrades
SW
NE
Pierre de Dijon-Corton
OUTER RAMP
INNER RAMP
MID-RAMP
OUTER RAMP
D- TST - Drowning (A/S>>>1; weak S and strong A)
Sequence VIII
Argiles de la Wöevre
about 20-30m sea level rise
shoal and lagoon transgress
Pierre de Dijon-Corton (Marnes à Eudesia)
SW
NE
marine phreatic zone
early lithification and marine bored surface
marine bored surface (SB8)
OUTER TO MID-RAMP
C- LST- exposure (A/S<0; low S and A<0) - forced regression
Sequence VIII
sea level fall 5-10 m
LST
exposure surface (SB8)
SW
NE
vadose zone
INNER RAMP
islands
oolitic shoal
Oolite de Fréville
LST
INNER RAMP
B- LATE HST - progradation (A/S<1; strong S and weak A)
Sequence VII
Calcaires de Chaumont
shoal progrades
SW
NE
zigzag to discus Zone
Oolite de Fréville
OUTER RAMP
Marnes à Rhynchonelles sup.
lagoon
island
lagoon
oolitic shoal
MID-RAMP
OUTER RAMP
INNER RAMP
A- EARLY HST - aggradation (A/S=1)
Sequence VII
Calcaires de Chaumont
Oolite de Fréville
SW
NE
zigzag to discus Zone
OUTER RAMP
Marnes à Rhynchonelles sup.
lagoon and shoal aggradate
lagoon
island
lagoon
oolitic shoal
MID-RAMP
OUTER RAMP
INNER RAMP

4.6. Clay mineralogy

Clay mineral assemblages are composed of chlorite, illite, kaolinite, random illite–smectite mixed layers (I/S) R0 (here called smectites) and random illite–smectite mixed layers R1 (Fig. 9G, Appendices C and D). Four intervals are distinguished:

- The Early Bajocian (*humphresianum* Zone) with relatively abundant kaolinite (20%), I/S R1 (30%) and illite (50%); (Fig. 9G). The higher proportions of kaolinite occur in eastern and southern parts of the Paris Basin (Appendix D).
- During the Late Bajocian, a mineralogical change occurred from kaolinite-rich to smectite-rich sediments. From the *niortense* to *parkinsoni* Zones, the clay fraction contains small amounts of kaolinite (<5%) balanced by the presence of smectite (20%). Proportions of illite and I/S R1 are similar to those from the Early Bajocian (Fig. 9).
- From the *morrisi* to the *discus* Zones, kaolinite proportions increase from 5% to 20% while smectite disappears (Fig. 9G). Kaolinite is more abundant in the eastern part of the Paris Basin than in its southern part (Appendix D).
- During the Early Callovian, clay assemblages are dominantly composed of illite and I/S R1 and kaolinite (20% on average). The proportions of this mineral decrease southwards from 30 to 40% in the north–east of the Paris basin to less than 5% in Burgundy (Appendix D).

5. Discussion: Factors controlling carbonate deposition

5.1. Accommodation and climatic changes—Global and regional trends

5.1.1. Eustasy vs European tectonic influences—A review

Sedimentary sequences and their system tracts are directly controlled by accommodation space (*A*) and by sediment supply (*S*) and/or carbonate production (*G*); (e.g. Schlager, 1993, 2005; Catuneanu et al., 2009). Accommodation space can be created by changes in (1) global eustasy (tectono-eustatism or glacio-eustatism) and/or (2) basin-scale subsidence rate which may be associated with local syn-sedimentary active faults. Changes in sediment supply and/or in carbonate production control the way the accommodation space is filled. Climatic changes and environmental effects at a global or regional scale are an important controlling factor of carbonate production and sediment supply. The TSTs previously recognized define a retrogradational geometry where S or $G<A$ (Schlager, 1993) whereas the HSTs reflect a progradational trend with S or $G>A$. In the eastern Paris Basin, the Middle Jurassic carbonate system displays variability on (1) geometries and (2) carbonate production and/or siliciclastic input. Detailed third-order cycles in the western Tethyan domain are well documented in Middle Jurassic European Basins (Dromart et al., 1996; Garcia et al., 1996a; Garcia et al., 1996b; Gaumet et al., 1996; Hardenbol et al., 1998; Gaumet et al., 2001). The 10 stratigraphic sequences recognized in this study compare well with the previously published cycles inferred from the north–west Tethyan domain (e.g. Hardenbol et al., 1998). The maximum flooding surfaces found in the northern Tethyan domain are also found in the eastern Paris Basin as the 'Vesulian transgression' which is well-expressed in Western Europe for the Late Bajocian (Figs 2 and 8); (Jacquin et al., 1998; Guillocheau et al., 2000; Aurell et al., 2003). This transgression is also recognized in Greenland (Surlyk, 1991), Argentina (Legarreta and Uliana, 1996), North Africa (Durlet et al., 2001a) and is considered as global by Hallam (2001).

The 10 third-order sequences recognized in this study represent a time interval of 8 My, corresponding to an average sequence duration of 0.8 My (Gradstein et al., 2004), that is in the duration range for third-order cycles (0.1 to 1 My; Schlager, 2005).

The origin of these cycles is still debated but relative sea-level changes represent the sum of (1) eustatic movements (tectono-eustasy and glacio-eustasy) and (2) regional tectonic movements (basin-scale subsidence). These cycles have been already interpreted as reflecting eustasy (Hardenbol et al., 1998). The main argument for this assumption is the success in global correlation of sequences and the similarity of the estimated sea level changes. In the west European domain, the Middle Jurassic is marked by (1) thermal doming in the central North Sea, (2) oceanic accretion in the Ligurian Tethys and (3) the opening of the Central Atlantic Ocean (Guillocheau et al., 2000). Added to the opening of Indian Oceans, these major geodynamic events which newly created ocean ridges displacing seawater onto continental margins, may control global-eustasy. European geodynamic events affecting the Eurasian plate may also control the thermal subsidence of the intracratonic Paris Basin which can be superimposed on global tectono-eustatic mechanisms (Guillocheau, 1991; Guillocheau et al., 2000; Robin et al., 2000). It is difficult to distinguish the relative role of tectono-eustasy and local basin subsidence because the two processes may have the same origin (Robin et al., 2000).

As suggested by Price (1999) for the Bathonian, eustasy can be influenced by the presence of ice (glacio-eustasy influence). In the eastern Paris Basin, whatever the origin of the third-order cycles, their successful global correlation at the European scale (Hardenbol et al., 1998), confirms the possible eustatic signal. Our study suggests that the maximum sea level fall inferred from the vertical occurrence of vadose cements was probably limited (5–10 m), while the sea level rise may have been of 50–100 m, judging from the presence of brachiopods, bivalves and crinoids in the marly interval of the Middle Jurassic outer ramp environment.

5.1.2. Western Europe palaeotemperature patterns

Previous studies have shown that marine bivalves precipitate their shells in oxygen isotope equilibrium with seawater (Mook and Vogel, 1968; Lécuyer et al., 2003), and their $\delta^{18}O$ values have been successfully used to reconstruct the sea surface temperatures (SST) of past oceans (Steuber et al., 2005; Brigaud et al., 2008), including for the Middle Jurassic (Anderson et al., 1994; Jenkyns et al., 2002; Wierzbowski and Joachimski, 2007). The *Trichites* and oyster shells that we recovered from the same stratigraphic levels display similar values (Appendix A), confirming the absence of vital effects for this group, at least for oxygen isotopes. Therefore we gathered the $\delta^{18}O$ from both organisms into a single data set to reconstruct the pattern of marine temperatures (Fig. 9). Throughout the whole study interval, we consider shallow palaeo-depths (<50 m for inner and mid-ramp), which allows us to reconstruct sea surface water temperatures from our $\delta^{18}O$ samples. A change from open to more restricted environments occurred during the Bathonian, with the development of a lagoon. However, the two Bathonian samples analysed come from an outer ramp environment, north of the lagoon. Consequently, all of our samples come from open marine environments. We used the equation of Anderson and Arthur (1983) to calculate marine temperatures from bivalve $\delta^{18}O$ values. A $\delta^{18}O$ of seawater of −1‰ SMOW is generally used for the Jurassic period, to account for the absence of ice-sheets (Shackleton and Kennett, 1975). However, in tropical areas, modern

Fig. 8. Diagram of facies/architecture changes at the Bathonian/Callovian transition in a third-order sequence stratigraphic framework. A—Early HST of Sequence VII is marked by lagoon and shoal aggradation in a muddy ramp. B—Carbonate production increased, and the ooid shoal progrates. C—Sea level fall caused a large exposure in the muddy ramp, with karstifications and vadose cementation. LST develops during sea level fall (*Oolite de Fréville*). D—The beginning of the TST is marked by marine bored surface during drowning, probably due to eustasy. TST (*Marnes à Eudesia*, *Marnes à Ornithella* and *Argiles de la Woëvre*) deposited in the entire study area. E—Carbonate production increased, and oobioclastic shoal progrades (HST).

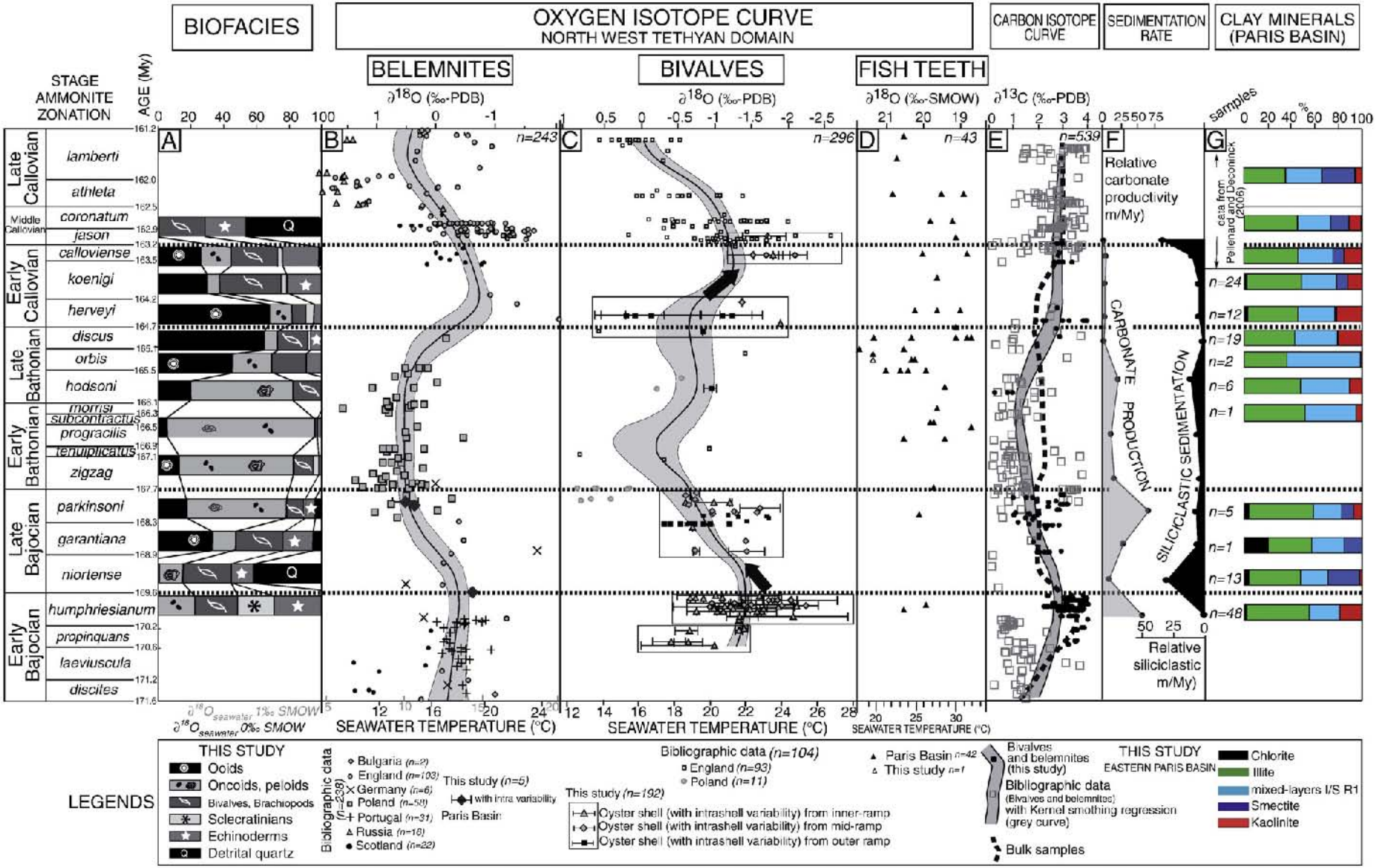

Fig. 9. A—Changes in biofacies associations during the Early Bajocian–Early Callovian interval. B–C–D—Evolution of Western Europe Peritethyan seawater temperatures during the Middle Jurassic period inferred (B) from belemnite rostra (this study and Anderson et al., 1994; Podlaha et al., 1998; Jenkyns et al., 2002; Wierzbowski and Joachimski, 2007; Metodiev and Koleva-Rekalova, 2008; Price and Page, 2008; Nunn et al., 2009) , (C) from bivalve shells (this study and Anderson et al., 1994; Jenkyns et al., 2002; Price and Page, 2008) and (D) from fish teeth (this study) and Lécuyer et al., 2003. Smoothing curves were computed using a Kernel Smoothing Regression, based on a Gaussian Kernel non-parametrical Regression (after Yi Cao available at http://www.mathworks.com/matlabcentral/fileexchange/19195). Grey area corresponds to the confidence interval of the smoothing curve. E—Carbon-isotope curve, data from this study, bivalve shells and belemnite rostra, and from bulk rocks (Corbin, 1994; Bartolini et al., 1999; Bartolini and Cecca, 1999; O'Dogherty et al., 2006). Grey curve is the Kernel smoothing interval confidence. F—Changes in carbonate production and in siliciclastic sedimentation rate in the eastern part of the Paris Basin. G—Changes in clay mineral assemblages. The graph indicates average clay proportions from samples of this study with bibliographic data correlated to ammonite biozonations and the geological time scale (Moral, 1979; Floquet et al., 1991; Javaux, 1992; Gradstein et al., 2004). Average proportions of clay minerals of the Middle and Late Callovian were computed using the HTM102 and A901 Andra boreholes (data from Pellenard and Deconinck, 2006).

surface waters are affected by intensified evaporation, which could result in an increase of 1‰ of the local seawater $\delta^{18}O$ compared with that of the global ocean (Zachos et al., 1994; Bigg and Rohling, 2000). We have therefore used a $\delta^{18}O$ seawater of 0‰ to reconstruct marine palaeotemperatures from our bivalve samples, which we think more appropriate for the relatively shallow environment (<50 m deep) and tropical latitudes of the study sections in the Middle Jurassic (Lécuyer et al., 2003; Pucéat et al., 2003; Roche et al., 2006).

Our data (192 *trichites* and oyster shells from the eastern Paris Basin) display a relatively large variability within the same stratigraphic interval (ammonite Zone), up to 8 °C, which is higher than the variability observed within a single oyster shell (2–3 °C on average, and up to 6 °C; Fig. 9). It is likely that this variability reflects seasonal changes in both temperature and seawater $\delta^{18}O$, although as shell growth may have slowed or ceased with extreme seasonal temperatures, we probably do not record the entire seasonal range (Brigaud et al., 2008). Despite this variability, our data display significant temperature changes within the study interval. A cooling of about 2 °C is recorded from temperatures of 22 °C on average during the Early Bajocian (*humphresianum* Zone) to 20 °C on average during the Late Bajocian (*garantiana and parkinsoni* Zones); (Fig. 9C). Our samples yield similar temperatures (19–20 °C) during the Late Bathonian and the earliest Callovian (Fig. 9C). A warming of about 4 °C is then observed from the earliest Callovian to the Early/Middle Callovian transition with temperatures reaching 24 °C on average (Fig. 9C).

We added to our new data set ($n=192$) a compilation of 104 $\delta^{18}O$ values for bivalves recovered from similar neritic environments of southern England and Poland (Anderson et al., 1994; Jenkyns et al., 2002; Wierzbowski and Joachimski, 2007; Price and Page, 2008). These data display variability comparable to our data, and also comparable temperatures as illustrated in the *jason* Zone (Fig. 9C). Poland oyster samples display lower temperatures of about 4 °C on average at the Bajocian/Bathonian transition (Wierzbowski and Joachimski, 2007). These lower temperatures may derive from the 5° higher palaeolatitude of Poland (30–35°N) compared with the Paris Basin or from the influence in this area of a cooler surface current from the boreal area at the onset of the Bathonian. As no data are available from the eastern Paris Basin at the beginning of the Bathonian (Fig. 9C), values coming from Polish sections could prolong the cooling trend initiated by our data from the lowermost Late Bajocian to the uppermost Late Bajocian (Fig. 9C). This remains to be confirmed by additional data from the Paris Basin or England. Data from England display a clear subsequent cooling of about 8 °C from the Early/Middle Callovian boundary (24 °C on average in the Paris Basin) to the end of the Callovian, with temperatures reaching a minimum of 16 °C in the *lamberti* Zone (Fig. 9C).

These sea surface temperature variations inferred from bivalve $\delta^{18}O$ values are not detected from fish-tooth $\delta^{18}O$ from the Paris Basin, except for the cooling trend of the Middle to Late Callovian (Dromart et al., 2003b; Lécuyer et al., 2003). The lack of higher fish-tooth $\delta^{18}O$ values during the Bajocian and Callovian may be due to the scarcity of available data. Some samples display markedly higher $\delta^{18}O$ values, and therefore lower temperatures, during the latest Bathonian. However, these samples are from the north-western Paris Basin which has been interpreted by Lécuyer et al. (2003) as evidence of a cooler water mass bathing the northern part of the Paris Basin.

Nevertheless, the temperature changes attested by bivalve $\delta^{18}O$ values are also recorded in belemnites. Add to our 3 belemnites, an exhaustive compilation of 238 belemnite oxygen isotope values is made (Fig. 9B) from England (Anderson et al., 1994; Jenkyns et al., 2002; Price and Page, 2008), Scotland (Jenkyns et al., 2002; Nunn et al., 2009), Portugal (Jenkyns et al., 2002), Bulgaria (Metodiev and Koleva-Rekalova, 2008), Poland (Wierzbowski and Joachimski, 2007), Germany (Podlaha et al., 1998) and Russia (Podlaha et al., 1998; Riboulleau et al., 1998). Temperatures have been calculated from belemnites using the equation of Anderson and Arthur (1983). Recent studies have suggested that belemnites were nectobenthic organisms, living close to the seafloor (Wierzbowski and Joachimski, 2007; Dera et al., 2009b; Wierzbowski and Joachimski, 2009). This interpretation can explain the lower temperature (2–3 °C) recorded in the 3 belemnites than those recorded in bivalves collected from a same stratigraphic level in the Pouillenay quarry. The coeval belemnites and bivalves are sampled in limestones and marls from the Pouillenay quarry (in F2 and F3 facies association) reflecting shallow environments of inner and mid-ramp (<50 m). The difference in $\delta^{18}O$ values may indicate that belemnites thrived in colder deeper water (basin), and could occasionally migrate to shallower and warmer waters (mid- to inner ramp). The temperatures inferred from contemporaneous belemnites from Portugal, England, Bulgaria, Germany, Scotland and the Paris Basin (e.g. in the Early Bajocian; Fig. 9C) are similar, although part of the belemnites from Scotland yield lower temperatures than the remainder of the samples. This suggests that bottom waters may have been well mixed in the Tethys. Belemnite $\delta^{18}O$ data display a cooling of Tethyan bottom waters from the Early Bajocian (*humphresianum* Zone) to the latest Bajocian (Fig. 9B), of similar amplitude (4 °C) to that recorded by the bivalves. Tethyan bottom temperatures remained quite stable, then, during the Early Bathonian. Data from the earliest Callovian are too scarce to distinguish whether the Early Callovian warming is also recorded by belemnites, although the few existing data yield higher temperatures than those from the earliest Late Bathonian (Fig. 9B). A cooling trend of about 6 °C is then suggested from the Middle to Late Callovian by belemnite $\delta^{18}O$ values, mirroring that evidenced by bivalve $\delta^{18}O$ from England (8 °C; Fig. 9B–C; Dromart et al., 2003a,b).

5.2. Climatic and eustatic influences on carbonate evolution

5.2.1. Vesulian unconformity: From bioclastic to ooid-dominated carbonate production (Early–Late Bajocian transition)

In Western Europe, the end of the Early Bajocian is usually marked by relatively high carbonate productivity (Dromart et al., 1996) with crinoid-rich facies and/or hermatypic coral reefs, in particular in the eastern Paris Basin (Geister and Lathuilière, 1991; Lathuilière, 2000a, b; Lathuilière and Marchal, 2009). At palaeolatitudes higher than 25–30°N, it was even the first time during the Mesozoic that scleractinian corals formed almost exclusively large reefs in shallow settings (Geister and Lathuilière, 1991; Leinfelder et al., 2002). Between reefs, the carbonate factory represented by echinoderms, brachiopods, bivalves and bryozoans suggests well-oxygenated water with normal salinity under oligo- to mesotrophic conditions (Piuz, 2004). Temperatures in western Tethyan seawater (18–28 °C) correspond to a maximal thermal event (*humphresianum* Zone; Fig. 9). This seawater temperature may have favoured the development of coral reefs in Western Europe in particular in the eastern Paris Basin.

In Middle Jurassic series of the eastern Paris Basin, the burial depth is relatively low and temperatures never exceed 50 °C (Clauer et al., 2007). As a result, in Mesozoic series, the clay mineralogical associations are generally considered as detrital and they can be used as an environmental proxy (Debrabant et al., 1992; Dera et al., 2009a). In the *humphriesianum* Zone (Early Bajocian), the kaolinite content reaching 15% may indicate either intensified chemical weathering of kaolinite soils or reworking of ancient kaolinite-bearing rocks (Chamley, 1989; Dera et al., 2009a). The occurrence of relatively abundant kaolinite in this interval is consistent with a warm climate suggested by isotopic data. Kaolinite may also indicate a more humid period (Fig. 10), as suggested by plant taxa (sphenophytes and pteridosperms) in England during the Early Bajocian in the Gristhorpe Member (Hesselbo et al., 2003).

A disturbance of the carbon cycle is evidenced in the Tethyan domain (Spain, France, Italy, England) by lighter carbon-isotope values at the Aalenian/Bajocian transition (Bartolini et al., 1999; Bartolini and Cecca, 1999; Hesselbo et al., 2003; O'Dogherty et al., 2006) followed by a positive carbon excursion at the end of the Early Bajocian (Corbin, 1994; Bartolini et al., 1999; Bartolini and Cecca,

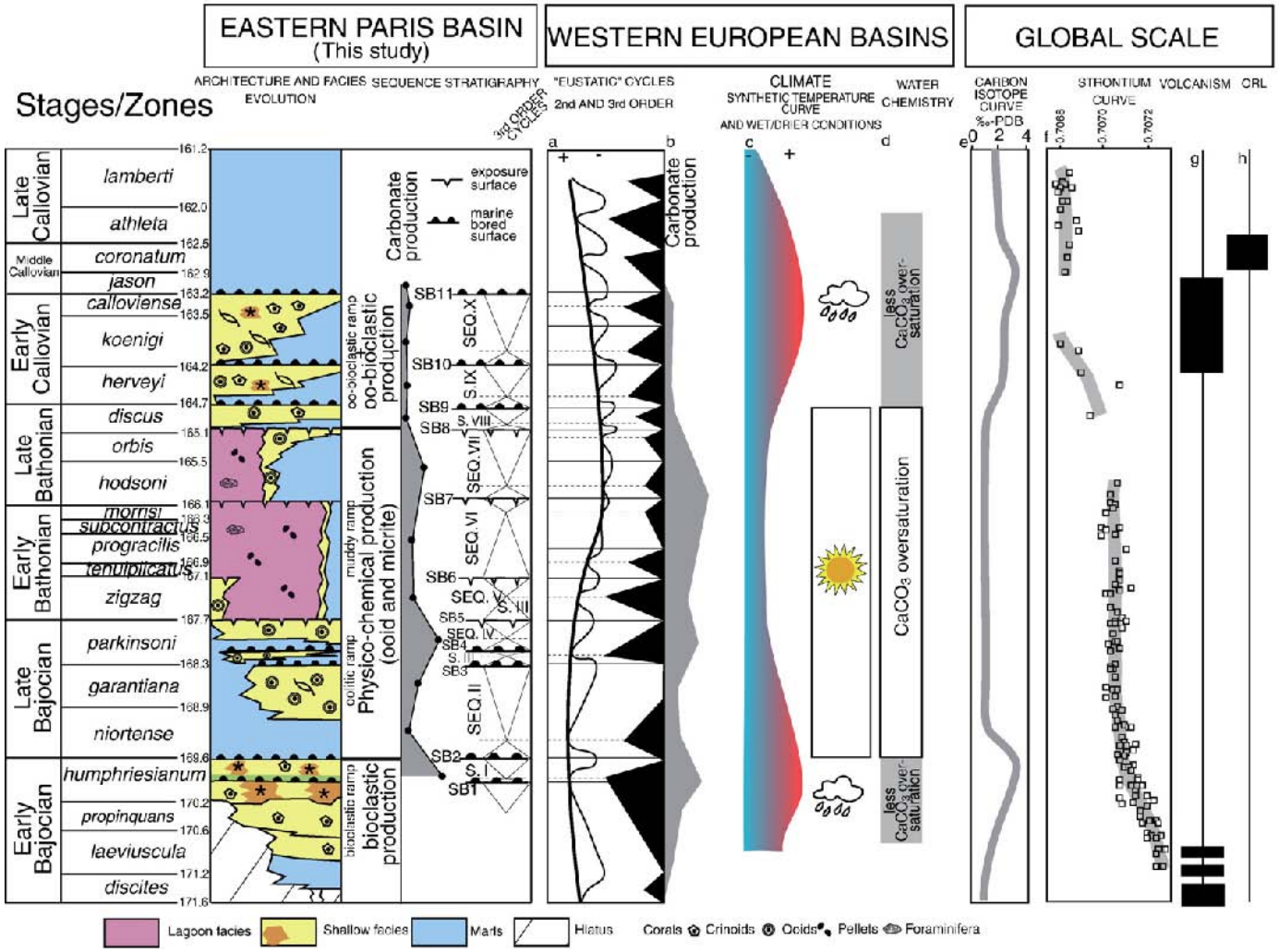

Fig. 10. Summary illustration of: —*The eastern Paris Basin* characteristics: main carbonate facies through time and environmental succession, sequences, 3rd order cycles, carbonate production; —The western European basins: A. eustatic cycles (Hardenbol et al., 1998); B. carbonate production (Dromart et al., 1996; Gaumet et al., 2001); C. synthetic palaeoclimate (data from Fig. 8) and D. water chemistry; —*The global scale*: E. carbon-isotope curve (from Fig. 8.); F. Strontium curve (Jones et al., 1994; Jenkyns et al., 2002), G. Circum-Pacific volcanism (Feraud et al., 1999; Pankhurst et al., 2000; Campbell et al., 2007) and H. organic rich layers (Dromart et al., 2003a).

1999; Morettini et al., 2002; O'Dogherty et al., 2006). Lighter carbon-isotope values indicate increased atmospheric pCO_2 whereas positive excursions correspond to reduced pCO_2 (e.g. Weissert and Mohr, 1996; Hesselbo et al., 2003). Bartolini and Cecca (1999), Bartolini and Larson (2001) and Hesselbo et al. (2003) interpret the $\delta^{13}C$ evolution as the result of increasing volcanism in circum-Pacific subduction zones which may have contributed to excess amounts of pCO_2 in the atmosphere. Following Bartolini and Cecca (1999), this increased pCO_2 may have affected seawater chemistry which would have caused a decrease in pH, coinciding with the onset of biosiliceous planktonic production and with a pelagic carbonate crisis in Italy during the Early Bajocian. Lowered oversaturation in calcium carbonate could explain the bioclastic composition of facies in neritic carbonate environments and explain the scarcity of physico-chemical precipitation (ooids, micrite) in Early Bajocian deposits of the Paris Basin (Fig. 10).

A drastic facies change underlain by the 'Vesulian' discontinuity (Durlet and Thierry, 2000) from bioclastic facies to marls/ooids facies occurred at the Early/Late Bajocian boundary in the Paris Basin. This change is also well-expressed in western Tethyan domains, for example in the Iberian domain at the Early/Late Bajocian boundary (from bioclastic facies to marls; Aurell et al., 2003) or in Switzerland (to ooid facies; Gonzalez, 1996; Gonzalez and Wetzel, 1996). It coincided with a sea level rise considered as global (Hallam, 2001) although other factors (climate) probably contributed to this crisis.

Seawater temperatures recorded in belemnites and bivalves show a decreasing trend in Western Europe. In the eastern Paris Basin, the clay mineralogy of Late Bajocian sediments reveals a dramatic mineralogical change characterized by the disappearance of kaolinite and the appearance of smectite (Fig. 9G). This change can be interpreted as indicative of cooler and drier conditions (Dera et al., 2009a). If clay minerals in the Paris Basin result from the erosion of palaeosols, the smectite may indicate high seasonal contrasts on continents (Chamley, 1989). Cooler conditions are consistent with temperatures as recorded by oxygen isotopes measured on belemnite guards and bivalves. A change from a wet to an arid environment is also suggested at the Early/Late Bajocian boundary (Fig. 10) with a microphyllous conifer floral assemblage becoming dominant during the Late Bajocian in the Scalby Formation, Yorkshire (Hesselbo et al., 2003). The mineralogical change may also reflect a eustatic rise of sea level with prevailing deposition of smectite in distal environments, while kaolinite was deposited in near-shore, proximal environments. The cooling episode of the Late Bajocian immediately following a $\delta^{13}C$ positive excursion, well-expressed both in marine domains (Corbin, 1994; Bartolini et al., 1999; Bartolini and Cecca, 1999; Morettini et al., 2002; O'Dogherty et al., 2006) and in terrestrial domain (Hesselbo et al., 2003), may indicate pumping of CO_2, inducing a decrease in atmospheric pCO_2 (Fig. 9E).

However, at present, marine organic carbon burial has not been found during the Bajocian (Bartolini et al., 1999). A similar situation is known also in the Valanginian where a positive $\delta^{13}C$ excursion is recorded although the organic matter storage in sediments is extremely limited (Gröcke et al., 2005). Additionally, the $^{87}Sr/^{86}Sr$ isotope curve plateau beginning at the Early/Late Bajocian transition can be interpreted as enhanced continental erosion and/or sea-floor activity decline (Fig. 10). This possible continental weathering may have induced a drop in pCO_2 which is consistent with a cooling episode. The climatic changes (cooling and drier conditions; Late Bajocian; Fig. 10) appear to be a major controlling factor in the shallow carbonate facies change from mainly bioclastic to ooid facies in Western Europe (Iberian domain, Paris Basin, Switzerland). An ammonite diversity crisis is also described for the Early/Late Bajocian transition (e.g. extinction of Stephanoceratoidea genus, O'Dogherty et al., 2006; Moyne and Neige, 2007). This possible drop in pCO_2 and drier conditions may have favoured carbonate calcium oversaturation in shallow carbonate environments, so enhancing ooid precipitation in seawater and possibly triggering the observed replacement of coral and bioclastic facies by ooids facies between the Early and the Late Bajocian.

5.2.2. Installation and development of a muddy ramp (Bathonian)

In the Paris Basin, large scale lagoon development in inner ramp environments occurred at the Bajocian/Bathonian boundary. This development corresponds to the maturity stage of the ooid ramp. The spatial distribution of oolitic shoals, formed in shallow, high-energy environments, show that they were localized and/or limited at the edge of fault structures (south of the Vittel Fault and north of the Neuchâteau fault; Fig. 4). At the beginning of the Bathonian, lagoonal environments were particularly well developed in this zone (Fig. 4). The local flexure movements related to influence of variscan accidents (e.g. Vittel Fault, Durlet et al., 1997; Jacquin et al., 1998) probably contribute to the installation of the protected inner ramp environments and to the polarity ramp flip-flopped (Fig. 4).

Sequence boundaries recording meteoric diagenesis and exposure episodes (SB5 to SB8), only observed during this period, are coeval with the minimum sea surface temperature in the western tethyan domain (Fig. 10). Glacio-eustasy may have influenced sea level drops during the Bathonian, with the possible ice presence at high palaeolatitudes (Price, 1999).

Ooid-rich carbonate deposits are also documented in the Iberian domain (Aurell et al., 2003) and England (Great Oolite, Sellwood et al., 1985). As in the pelagic domain of Spain and Italy, there is no significant carbon-isotope change at the Bajocian/Bathonian boundary and during the Bathonian (Fig. 9, Bartolini et al., 1999; O'Dogherty et al., 2006), suggesting stable environmental conditions and relatively low pCO_2. The $^{87}Sr/^{86}Sr$ isotope curve is also stable from the beginning of the Late Bajocian to the Late Bathonian (Fig. 10), suggesting possible stable conditions. Stable and low pCO_2 conditions may have favoured calcium carbonate oversaturation, carbonate precipitation, and the development of this muddy ramp in the eastern part of the Paris Basin.

5.2.3. The origin of carbonate depletion at the Bathonian/Callovian boundary

A major carbonate productivity crisis and a decrease in the ooid/(bivalve plus echinoderm) ratio are observed at the Bathonian/Callovian boundary. This waning of carbonate production at the Bathonian/Callovian boundary is observed from England (Bradshaw and Cripps, 1992; Jeans, 2006) to the Iberian domain (Aurell et al., 2003) and is well documented by Dromart et al. (1996) and Gaumet et al. (2001). The seawater temperature shows a warming during the Early Callovian, peaking at the Early/Middle Callovian boundary. This change, which follows an increase in kaolinite (Fig. 9G), observed as soon as the Late Bathonian in the northern Paris Basin and England (Debrabant et al., 1992; Jeans, 2006), may indicate enhanced weathering in a warm and humid climate (Chamley, 1989). Vascular plant biomarkers used as proxies for palaeoflora and palaeflora indicate also humid conditions during the Callovian in the Eastern Paris Basin (Hautevelle et al., 2006). The circum-Pacific volcanism active during the Early Callovian may have contributed to the rise in pCO_2 (Dromart et al., 2003a; Campbell et al., 2007). Consequently, high pCO_2 levels may have enhanced weathering, resulting in high nutrient transfer to the oceans (e.g. Weissert and Mohr, 1996). Together with eutrophic conditions and greater detrital input in a humid climate, the rise in pCO_2 favoured lowered oversaturation in calcium carbonate (ocean acidification), possibly explaining the widespread neritic carbonate production crisis in Western Europe and the Arabian domain (Dromart et al., 2003a). The coeval second-order global sea level rise during the Callovian may also have enhanced the carbonate crisis (Hardenbol et al., 1998; Pellenard et al., 1999). Widespread eutrophication of seawater seems to become favourable to organic carbon burial during the earliest Middle Callovian (organic rich layer in the central Atlantic and in the western Tethyan domain during the Middle Callovian; Bartolini et al., 1999; Dromart et al., 2003a). This scenario, although still speculative, is confirmed by the $\delta^{13}C$ increase from the latest Early Callovian to the Middle Callovian (Fig. 10). Seawater cooling during the Middle–Late Callovian following the

carbonate crisis, can be related to this carbon sequestration during the Middle Callovian (Dromart et al., 2003a,b).

6. Conclusions

The Middle Jurassic formations consist of 18 lithofacies attributed to five major facies associations that are characteristic of distinct carbonate ramp settings. Four biosedimentary packages can be distinguished during the Early Bajocian–Early Callovian, characterized by distinct allochem associations and sedimentary architectures. (1) A large intracratonic carbonate environment with coral reefs and bioclast-rich facies characterized the Early Bajocian. (2) A major facies change occurred at the Early/Late Bajocian boundary (Vesulian unconformity) with development of clay-rich and ooid-rich facies deposited in a southward-dipping ramp. (3) The Bathonian period is marked by the development of a large protected inner ramp environment (lagoonal, intertidal and supratidal facies) developed in the Paris Basin (Figs. 1, 4 and 5), the ooid shoal prograded favouring the development of a wide lagoon with infratidal to supratidal environments. (4) At the Bathonian/Callovian boundary, a second major change occurred with the waning of lagoonal facies replaced by an ooid-bioclastic ramp associated with a waning of carbonate productivity (retrogradational trend). Ten depositional sequences are identified in carbonate formations of the eastern part of the Paris Basin. They reflect third-order sequences relative to sea-level variations.

Palaeotemperature reconstructions inferred from $\delta^{18}O$ of bivalve shells and belemnite rostra allow us to refine existing sea surface palaeotemperature patterns. This is the first time that a cooling from the latest Early Bajocian to the Late Bajocian and a subsequent warming from the earliest Callovian to the Early/Middle Callovian boundary has been described using a proxy of sea surface temperatures. Together with $\delta^{13}C$, mineralogical data and compilation of palaeotemperature data from the western Tethys, our new palaeotemperature values suggest the palaeo-climatic/palaeo-environmental controls of facies on a shallow carbonate ramp environment. The high carbonate production with coral-reef development during the Early Bajocian was clearly optimized by warm conditions. Possible high pCO_2 and associated lowered oversaturation in calcium carbonate probably favoured only bioclasts as carbonate producers, impeding ooid and micrite precipitation. Environmental changes to cooler and drier conditions, suggested by $\delta^{18}O$ and clay mineral assemblages occurred at the Early/Late Bajocian. The Late Bajocian cooling episode immediately following a positive $\delta^{13}C$ excursion may indicate pumping of CO_2. Drier conditions associated with a fall in pCO_2 may have favoured calcium carbonate oversaturation in seawater which could have triggered the observed replacement of bioclastic and coral facies by ooid facies in Western Europe. At the Bajocian/Bathonian boundary, the appearance of a wide lagoon corresponds to the maturity stage of the previous ooid ramp. A muddy ramp developed in a large part of the Paris Basin. The relatively stable climatic conditions and carbon cycle may also have favoured carbonate production in oversatured seawater. Exposure episodes, only observed during the Bathonian period, are coeval with the minimum sea surface temperature in the western tethyan domain. Glacio-eustasy may have influenced sea level drops during the Bathonian, with the possible ice presence at high palaeolatitudes (Price, 1999). Climate warming, possibly related to volcanism (increase pCO_2) favoured eutrophic conditions and lowered oversaturation which could explain the widespread carbonate production crisis in Western Europe. Seawater cooling during the Middle/Late Callovian interval followed this carbonate crisis.

Acknowledgements

This study is supported by an Andra (French agency for radioactive waste management) PhD grant. We thank Philippe Courville for brachiopod determinations. We would like to thank Pascal Taubaty for the quality of the thin sections, Claude Aurière for providing the samples from the core storage (Bure site), Guillaume Charbonnier, Cristina Constantin and Kevin Dinzambou for their help in sample preparations, and Nathalie Guichard for her assistance during the XRD analyses. We also acknowledge the guidance of Rémi Laffont and Fabrice Monna in statistic treatments of isotopic data. We are grateful to TOTAL for allowing us access to the L.LI.CD.1 cores (special thanks to Catherine Javaux, Guy Nesen, and Daniel Monge; Boussens site). This paper benefited from the constructive reviews of B. Pratt and an anonymous reviewer.

Appendices A, B, C and D. Supplementary data

Supplementary data associated with this article can be found, in the online version, at doi:10.1016/j.sedgeo.2009.09.005.

References

Anderson, T.F., Arthur, M.A., 1983. Stable isotopes of oxygen and carbon and their application to sedimentologic and paleonvironmental problems. Stable Isotopes in Sedimentary Geology: In: Arthur, M.A., Anderson, T.F., Kaplan, I.R., Veizer, J., Land, L.S. (Eds.), Society of Economic Paleontologists and Mineralogists Short Course, vol. 10, pp. 1–151.

Anderson, T.F., Popp, B.N., Williams, A.C., Ho, L.Z., Hudson, J.D., 1994. The stable isotopic records of fossils from the Peterborough Member, Oxford Clay Formation (Jurassic), UK: paleoenvironmental implications. Journal of the Geological Society (London, United Kingdom) 151, 125–138.

Aurell, M., Robles, S., Bádenas, B., Rosales, I., Quesada, S., Meléndez, G., García-Ramos, J.C., 2003. Transgressive–regressive cycles and Jurassic palaeogeography of northeast Iberia. Sedimentary Geology 162, 239–271.

Bartolini, A., Baumgartner, P.O., Guex, J., 1999. Middle and Late Jurassic radiolarian palaeoecology versus carbon-isotope stratigraphy. Palaeogeography, Palaeoclimatology, Palaeoecology 145, 43–60.

Bartolini, A., Cecca, F., 1999. 20 My hiatus in the Jurassic of Umbria–Marche Apennines (Italy): carbonate crisis due to eutrophication. Comptes Rendus de l'Académie des Sciences Serie II Fascicule a–Sciences de la Terre et des Planètes 329, 587–595.

Bartolini, A., Larson, R.L., 2001. Pacific microplate and the Pangea supercontinent in the Early to Middle Jurassic. Geology 29, 735–738.

Bigg, G.R., Rohling, E.J., 2000. An oxygen isotope data set for marine waters. Journal of Geophysical Research—Oceans 105, 8527–8535.

Bradshaw, M.J., Cripps, D.W., 1992. Jurassic. Atlas of Palaeogeography and Lithofacies. In: Cope, J.C.W., Ingham, J.K., Rawson, P.F. (Eds.), Memoirs, vol. 13. Geological Society of London, p. 153.

Brigaud, B., Pucéat, E., Pellenard, P., Vincent, B., Joachimski, M.M., 2008. Climatic fluctuations and seasonality during the Late Jurassic (Oxfordian–Early Kimmeridgian) inferred from $\delta^{18}O$ of Paris Basin oyster shells. Earth and Planetary Science Letters 273, 58–67.

Brigaud, B., Durlet, C., Deconinck, J.-F., Vincent, B., Thierry, J., Trouiller, A., 2009. The origin and timing of multiphase cementation in carbonates: impact of regional scale geodynamic events on the Middle Jurassic Limestones diagenesis (Paris Basin, France). Sedimentary Geology 222, 161–180.

Burchette, T.P., Wright, V.P., 1992. Carbonate ramp depositional systems. Sedimentary Geology 79, 3–57.

Campbell, S.D.G., Sewell, R.J., Davis, D.W., So, A.C.T., 2007. New U–Pb age and geochemical constraints on the stratigraphy and distribution of the Lantau Volcanic Group, Hong Kong. Journal of Asian Earth Sciences 31, 139–152.

Catuneanu, O., Abreu, V., Bhattacharya, J.P., Blum, M.D., Dalrymple, R.W., Eriksson, P.G., Fielding, C.R., Fisher, W.L., Galloway, W.E., Gibling, M.R., Giles, K.A., Holbrook, J.M., Jordan, R., Kendall, C.G.S.C., Macurda, B., Martinsen, O.J., Miall, A.D., Neal, J.E., Nummedal, D., Pomar, L., Posamentier, H.W., Pratt, B.R., Sarg, J.F., Shanley, K.W., Steel, R.J., Strasser, A., Tucker, M.E., Winker, C., 2009. Towards the standardization of sequence stratigraphy. Earth-Science Reviews 92, 1–33.

Chamley, H., 1989. Clay Sedimentology. Springer Verlag. 623 pp.

Clauer, N., Fourcade, S., Cathelineau, M., Girard, J.-P., Vincent, B., Elie, M., Buschaert, S., Rousset, D., 2007. A review of studies on the diagenetic evolution of the Dogger to Tithonian sedimentary-sequence in the eastern Paris Basin—impact on the physical and chemical rock properties. Mémoire de la Société géologique de France 178, 59–71.

Collin, P.-Y., Courville, P., 2006. Sedimentation and palaeogeography of the eastern part of the Paris Basin (France) at the Middle–Upper Jurassic boundary. Comptes Rendus Geosciences 338, 824–833.

Collin, P.Y., Courville, P., Loreau, J.P., Marchand, D., Thierry, J., 1999. Condensed series and biostratigraphic unit preservation index: example of the flooding of the north Burgundy platform (France) in Callovian–Oxfordian times. Comptes Rendus De L Academie Des Sciences Serie Ii Fascicule a-Sciences De La Terre Et Des Planetes 328, 105–111.

Collin, P.Y., Loreau, J.P., Courville, P., 2005. Depositional environments and iron ooid formation in condensed sections (Callovian–Oxfordian, south-eastern Paris Basin, France). Sedimentology 52, 969–985.

Contini, 1968. Stratigraphie du Dogger: passage des faciès de la Haute-Saône aux faciès de Lorraine. Bulletin de la Société Géologique de France 10, 308–315.

Corbin, J.-C., 1994. Evolution géochimique du Jurassique du Sud-Est de la France: influence des variations du niveau marin et de la tectonique. PhD thesis, Université Paris VI, 175 pp.

Courville, P., Raffray, M., 2007. La série condensée à ("Marno-calcaires à Oolites ferrugineuses", Callovien pars.) de Rimaucourt (Haute-Marne). Lithologie, datation, aspects paléoenvironnementaux. Bulletin de l'Association Géologique Auboise 28, 3–12.

Debrabant, P., Chamley, H., Deconinck, J.-F., Récourt, P., Trouiller, A., 1992. Clay sedimentology, mineralogy and chemistry of Mesozoic sediments drilled in the Northern Paris Basin. Scientific Drilling 3, 138–152.

Dera, G., Pellenard, P., Neige, P., Deconinck, J.-F., Pucéat, E., Dommergues, J.-L., 2009a. Distribution of clay minerals in Early Jurassic Peritethyan seas: palaeoclimatic significance inferred from multiproxy comparisons. Palaeogeography, Palaeoclimatology, Palaeoecology 271, 39–51.

Dera, G., Pucéat, E., Pellenard, P., Neige, P., Delsate, D., Joachimski, M.M., Reisberg, L., Martinez, M., 2009b. Water mass exchange and variations in seawater temperature in the NW Tethys during the Early Jurassic: evidence from neodymium and oxygen isotopes of fish teeth and belemnites. Earth and Planetary Science Letters, 286, 198-207.

Dromart, G., Allemand, P., Garcia, J.P., Robin, C., 1996. Cyclic fluctuation of carbonate production through the Jurassic along a Burgundy–Ardeche cross-section, eastern France. Bulletin de la Société Géologique de France 167, 423–433.

Dromart, G., Garcia, J.-P., Gaumet, F., Picard, S., Rousseau, M., Atrops, F., Lecuyer, C., Sheppard, S.M.F., 2003a. Perturbation of the carbon cycle at the Middle/Late Jurassic transition: geological and geochemical evidence. American Journal of Science 303, 667–707.

Dromart, G., Garcia, J.P., Picard, S., Atrops, F., Lécuyer, C., Sheppard, S.M.F., 2003b. Ice age at the Middle–Late Jurassic transition? Earth and Planetary Science Letters 213, 205–220.

Durlet, C., Jacquin, T., Floquet, M., 1997. Extensional synsedimentary tectonics during Aalenian and Bajocian on the Burgundy High (France). Comptes Rendus de l'Académie des Sciences Série IIa:Sciences de la Terre et des Planètes 324, 1001–1008.

Durlet, C., Thierry, J., 2000. Modalités séquentielles de la transgression aalénobajocienne sur le sud-est du Bassin parisien. Bulletin de la Société Géologique de France 171, 327–339.

Durlet, C., Almeras, Y., Chellai, E.H., Elmi, S., Le Callonnec, L., Lezin, C., Neige, P., 2001a. Anatomy of a Jurassic carbonate ramp: a continuous outcrop transect across southern margin of the High Atlas (Morocco). Géologie Méditerranéenne 28, 57–61.

Durlet, C., Lathuilière, B., Aycard, M., 2001b. Reef geometries and facies in Bajocian limestones of the Burgundy High (France): environmental and sequence stratigraphy interpretations. Eclogae Geologicae Helvetiae 94, 1–11.

Enay, R., Mangold, C., 1980. Synthèse paléogéographique du Jurassique français, Document du Laboratoire de Géologie de Lyon, Volume 5. Groupe Français d'Etude du Jurassique. 220 pp.

Faber, J., 1957. Dossier de fin de campagne core-drills—Société Nationale des Pétroles d'Aquitaine. Bureau Exploration-Production des Hydrocarbures rapport n°14.1306–1312, Direction des Ressources Énergétiques et Minérales.

Feraud, G., Alric, V., Fornari, M., Bertrand, H., Maller, M., 1999. 40Ar/39Ar dating of the Jurassic volcanic province of Patagonia: migrating magmatism related to Gondwana break-up and subduction. Earth and Planetary Science Letters 172, 83–96.

Ferry, S., Pellenard, P., Collin, P.Y., Thierry, J., Marchand, D., Deconinck, J.F., Robin, C., Carpentier, C., Durlet, C., Curial, A., 2007. Synthesis of recent stratigraphic data on Bathonian to Oxfordian deposits of the eastern Paris Basin. Mémoire de la Société Géologique de France 178, 37–57.

Floquet, M., Laurin, B., Laville, P., Marchand, D., Menot, J.-C., Pascal, A., Thierry, J., 1989. Les systèmes sédimentaires bourguignons d'âge Bathonien Terminal–Callovien. Bulletin Centres de Recherches Exploration–Production Elf Aquitaine 13, 133–165.

Floquet, M., Javaux, C., Menot, J.-C., Purser, B.H., 1991. Sédimentation, diagenèse et séquences de dépôt dans les séries carbonatées de plate-forme d'âge Bathonien à Oxfordien en Bourgogne. excursion des 27–28–29 juin 1991, 14. ASF. 174 pp.

Flügel, E., 2004. Microfacies of Carbonate Rocks. Analysis, Interpretation and Application. Springer. 976 pp.

Garcia, J.-P., Dromart, G., Guillocheau, F., Allemand, P., Gaumet, F., Robin, C., Sambet, G., 1996a. Bathonian–Callovian Paris Basin–Subalpine Basin intercorrelations along an Ardennes–Ardèche cross-section. Comptes Rendus de l'Académie des Sciences Serie II Fascicule a-Sciences de la Terre et des Planètes 323, 697–703.

Garcia, J.-P., Laurin, B., Sambet, G., 1996b. Les associations de brachiopodes du Jurassique moyen du bassin de Paris; une échelle biochronologique ponctuée de niveaux-repères pour la contrainte des corrélations séquentielles à haute résolution. Bulletin de la Société géologique de France 167, 435–451.

Gaumet, F., Garcia, J.P., Dromart, G., Sambet, G., 1996. Stratigraphic control upon depositional facies, geometries and profiles across the Bathonian–Callovian carbonate platform in Burgundy. Bulletin de la Société géologique de France 167, 409–421.

Gaumet, F., 1997. Fondements géologiques pour la modélisation stratigraphique des systèmes carbonatés. Le Jurassique moyen de l'Angleterre à la Méditerranée. PhD thesis, Université Claude Bernard—Lyon I, 296 pp.

Gaumet, F., Garcia, J.P., Dromart, G., Allemand, P., 2001. Middle Jurassic production rates and "patchy" architecture of the carbonate systems along the north-western Tethyan margin (Paris basin to Sub-alpine basin): Géologie Méditerranéenne, vol. XXVIII, pp. 79–83.

Geister, J., Lathuilière, B., 1991. Jurassic coral reefs of the northeastern Paris Basin (Luxembourg and Lorraine), International Symposium on Fossil Cnidaria: Excursion-Guidebook VI, Münster, p. 112.

Gonzalez, R., 1996. Response of shallow-marine carbonate facies to third-order and high-frequency sea-level fluctuations: Hauptrogenstein formation, northern Switzerland. Sedimentary Geology 102, 111–130.

Gonzalez, R., Wetzel, A., 1996. Stratigraphy and paleogeography of the Hauptrogenstein and Klingnau Formations (middle Bajocian to late Bathonian), northern Switzerland. Eclogae Geologicae Helvetiae 89, 695–720.

Gradstein, F.M., Ogg, J.G., Smith, A.G., 2004. A Geological Time Scale 2004. Cambridge University Press.

Gröcke, D.R., Price, G.D., Robinson, S.A., Baraboshkin, E.Y., Mutterlose, J., Ruffell, A.H., 2005. The Upper Valanginian (Early Cretaceous) positive carbon-isotope event recorded in terrestrial plants. Earth and Planetary Science Letters 240, 495–509.

Guillocheau, F., 1991. Large-scale transgressive-regressive cycles of tectonic origin into the mesozoic sediments of the paris basin. Comptes Rendus de l'Academie des Sciences Serie II Fascicule a-Sciences de la Terre et des Planetes 312, 1587–1593.

Guillocheau, F., Robin, C., Allemand, P., Bourquin, S., Brault, N., Dromart, G., Friedenberg, R., Garcia, J.-P., Gaulier, J.-M., Gaumet, F., Grosdoy, B., Hanot, F., le Strat, P., Mettraux, M., Nalpas, T., Prija, C., Rigollet, C., Serrano, O., Grandjean, G., 2000. Meso-Cenozoic geodynamic evolution of the Paris Basin: 3D stratigraphic constraints. Geodinamica Acta 13, 189–245.

Guillocheau, F., Robin, C., Mettraux, M., Dagallier, G., Robin, F.-X., Le Solleuz, A., 2002. Le Jurassique de l'Est du Bassin de Paris. Bulletin d'information des Géologues du Bassin de Paris 39, 23–47.

Hallam, A., 2001. A review of the broad pattern of Jurassic sea-level changes and their possible causes in the light of current knowledge. Palaeogeography, Palaeoclimatology, Palaeoecology 167, 23–37.

Hardenbol, J., Thierry, J., Farley, M.B., Jacquin, T., de Graciansky, P.-C., Vail, P.R., 1998. Jurassic sequence chronostratigraphy—Chart 6. Mesozoic and Cenozoic Sequence Stratigraphy of European Basins: In: De Graciansky, P.-C., Hardenbol, J., Jacquin, T., Vail, P.-R. (Eds.), SEPM Special Publication, vol. 60, pp. 3–15.

Hautevelle, Y., Michels, R., Malartre, F., Trouiller, A., 2006. Vascular plant biomarkers as proxies for palaeoflora and palaeoclimatic changes at the Dogger/Malm transition of the Paris Basin (France). Organic Geochemistry 37, 610–625.

Hesselbo, S.P., Morgans-Bell, H.S., McElwain, J.C., Rees, P.M., Robinson, S.A., Ross, C.E., 2003. Carbon-cycle perturbation in the Middle Jurassic and accompanying changes in the terrestrial paleoenvironment. Journal of Geology 111, 259–276.

Holtzapffel, 1985. Les minéraux argileux. Préparation. Analyse diffractométrique et détermination, 12. Société Géologique du Nord. 136 pp.

Jacquin, T., de Graciansky, P.-C., 1998. Major transgressive/regressive cycles: the stratigraphic signature of european basin development. Mesozoic and Cenozoic Sequence Stratigraphy of European Basins: In: De Graciansky, P.-C., Hardenbol, J., Jacquin, T., Vail, P.R. (Eds.), SEPM Special publication No. 60, pp. 15–29.

Jacquin, T., Dardeau, G., Durlet, C., de Graciansky, C., Hantzpergue, P., 1998. The north sea cycle: an overview of 2nd-order transgressive/regressive facies cycles in western europe. Mesozoic and Cenozoic Sequence Stratigraphy of European Basins: In: de Graciansky, P.-C., Hardenbol, J., Jacquin, T., Vail, P.R. (Eds.), SEPM Special publication No. 60, pp. 445–466.

Javaux, C., 1992. La plate-forme parisienne et bourguignonne au Bathonien terminal et au Callovien—Dynamique sédimentaire, séquentielle et diagénétique, Place et création des réservoirs potentiels, 16. Mémoires géologiques de l'Université de Dijon, Dijon. 342 pp.

Jeans, C.V., 2006. Clay mineralogy of the Jurassic strata of the British Isles. Clay Minerals 41, 187–307.

Jenkyns, H.C., Jones, C.E., Gröcke, D.R., Hesselbo, S.P., Parkinson, D.N., 2002. Chemostratigraphy of the Jurassic System: applications, limitations and implications for palaeoceanography. Journal of the Geological Society 159, 351–378.

Jones, C.E., Jenkyns, H.C., Coe, A.L., Hesselbo, S.P., 1994. Strontium isotopic variations in Jurassic and Cretaceous seawater. Geochimica et Cosmochimica Acta 58, 3061–3074.

Lathuilière, B., 2000a. Reef building corals of Lower Bajocian of France. Part 1. Geobios 33, 51–72.

Lathuilière, B., 2000b. Reef building corals of Lower Bajocian of France (part 2). Geobios 33, 153–181.

Lathuilière, B., Marchal, D., 2009. Extinction, survival and recovery of corals from the Triassic to Middle Jurassic time. Terra Nova 21, 57–66.

Lathuilière, B., Gaillard, C., Habrant, N., Bodeur, Y., Boullier, A., Enay, R., Hanzo, M., Marchand, D., Thierry, J., Werner, W., 2005. Coral zonation of an Oxfordian reef tract in the northern French Jura. Facies 50, 545–559.

Laville, P., Cussey, R., Durand, J., Floquet, M., 1989. Faciès, structure et dynamique de mise en place de dunes oobioclastiques au Callovien inférieur en Bourgogne. Bulletin Centres de Recherches Exploration–Production Elf Aquitaine 13, 379–393.

Lécuyer, C., Picard, S., Garcia, J.-P., Sheppard, S.M.F., Grandjean, P., Dromart, G., 2003. Thermal evolution of Tethyan surface waters during the Middle–Late Jurassic: evidence from $\delta^{18}O$ values of marine fish teeth. Paleoceanography 18, 1076.

Legarreta, L., Uliana, M.A., 1996. The Jurassic succession in west–central Argentina: stratal patterns, sequences and paleogeographic evolution. Palaeogeography, Palaeoclimatology, Palaeoecology 120, 303–330.

Leinfelder, R.R., Schmid, D.U., Nose, M., Werner, W., 2002. Jurassic reef patterns—the expression of a changing globe. Phanerozoic Reef Patterns: In: Kiessling, W., Flügel, E., Golonka, J. (Eds.), SEPM Special Publication 72, vol. 72, pp. 465–520.

Lemoigne, Y., Thierry, J., 1968. La paléoflore du Jurassique moyen de Bourgogne. Bulletin de la Société géologique de France 7, 323–333.

Loreau, J.P., 1982. Sédiments aragonitiques et leur genèse. Mémoire Museum National Histoire Naturelle, vol. 47. Editions du Museum. 307 pp.

Mangold, C., Poirot, E., Lathuilière, B., Le Roux, J., 1994. Biochronologie du Bajocien supérieur et du Bathonien de Lorraine (France). Geobios M.S. 17, 343–349.

Metodiev, L., Koleva-Rekalova, E., 2008. Stable isotope records ($\delta^{18}O$ and $\delta^{13}C$) of Lower–Middle Jurassic belemnites from the Western Balkan mountains (Bulgaria): palaeoenvironmental application. Applied Geochemistry 23, 2845–2856.

Mook, W.G., Vogel, J.C., 1968. Isotopic equilibrium between shells and their environment. Science 159, 874–875.
Moore, D.M., Reynolds, R.C., 1989. X-ray Diffraction and the Identification and Analysis of Clay Minerals. Oxford University Press, New York. 332 pp.
Moral, P., 1979. Contribution à l'étude des matériaux détritiques dans la formation calcaire du Bajocien à l'Ouest de Dijon. PhD thesis, Université de Bourgogne, Dijon, 151 pp.
Morettini, E., Santantonio, M., Bartolini, A., Cecca, F., Baumgartner, P.O., Hunziker, J.C., 2002. Carbon isotope stratigraphy and carbonate production during the Early–Middle Jurassic: examples from the Umbria–Marche–Sabina Apennines (central Italy). Palaeogeography, Palaeoclimatology, Palaeoecology 184, 251–273.
Moyne, S., Neige, P., 2007. The space–time relationship of taxonomic diversity and morphological disparity in the Middle Jurassic ammonite radiation. Palaeogeography, Palaeoclimatology, Palaeoecology 248, 82–95.
Nunn, E.V., Price, G.D., Hart, M.B., Page, K.N., Leng, M.J., 2009. Isotopic signals from Callovian–Kimmeridgian (Middle–Upper Jurassic) belemnites and bulk organic carbon, Staffin Bay, Isle of Skye, Scotland. Journal of the Geological Society, London 166, 633–641.
O'Dogherty, L., Sandoval, J., Bartolini, A., Bruchez, S., Bill, M., Guex, J., 2006. Carbon-isotope stratigraphy and ammonite faunal turnover for the Middle Jurassic in the Southern Iberian palaeomargin. Palaeogeography, Palaeoclimatology, Palaeoecology 239, 311–333.
Pankhurst, R.J., Riley, T.R., Fanning, C.M., Kelley, S.P., 2000. Episodic silicic volcanism in Patagonia and the Antarctic Peninsula: chronology of magmatism associated with the break-up of Gondwana. Journal of Petrology 41, 605–625.
Pellenard, P., Deconinck, J.F., 2006. Mineralogical variability of Callovo-Oxfordian clays from the Paris Basin and the Subalpine Basin. Comptes Rendus Geoscience 338, 854–866.
Pellenard, P., Deconinck, J.-F., Marchand, D., Thierry, J., Fortwengler, D., Vigneron, G., 1999. Contrôle géodynamique de la sédimentation argileuse du Callovien-Oxfordien moyen dans l'Est du bassin de Paris : influence eustatique et volcanique. Comptes Rendus de l'Académie des Sciences Série II Fascicule a-Sciences de la Terre et des Planètes 328, 807–813.
Pierre, A., Durlet, C., Razin, P. and Chellai, E.H., in press. Spatial and temporal distribution of ooids along a Jurassic carbonate ramp: data from a continuous outcrop transect across the High-Atlas of Morocco. In: F.S.P. van Buchem, K. Gerdes and M. Esteban (Editors), Mesozoic and Cenozoic carbonate systems of the Mediterranean and the Middle East - stratigraphic and diagenetic reference models -. The Geological Society London. Special Publication.
Piuz, A., 2004. Micropaléontologie d'une plate-forme bioclastique échinodermique : Les calcaires à entroques du Bajocien du Jura méridional et de Bourgogne., 49. PhD Thesis. Université de Genève, 267 pp.
Podlaha, O.G., Mutterlöse, J., Veizer, J., 1998. Preservation of delta O-18 and delta C-13 in belemnite rostra from the Jurassic Early Cretaceous successions. American Journal of Science 298, 534.
Price, G.D., 1999. The evidence and implications of polar ice during the Mesozoic. Earth-Science Reviews 48, 183–210.
Price, G.D., Page, K.N., 2008. A carbon and oxygen isotopic analysis of molluscan faunas from the Callovian–Oxfordian boundary at Redcliff Point, Weymouth, Dorset: implications for belemnite behaviour. Proceedings of the Geologist's Association 119, 153–160.
Pucéat, E., Lécuyer, C., Sheppard, S.M.F., Dromart, G., Reboulet, S., Grandjean, P., 2003. Thermal evolution of Cretaceous Tethyan marine waters inferred from oxygen isotope composition of fish tooth enamels. Paleoceanography 18, 1029–1040.
Purser, B.H., 1969. Syn-sedimentary marine lithification of Middle Jurassic in the Paris Basin. Sedimentology 12, 205–230.
Purser, B.H., 1975. Sédimentation et diagenèse précoce des séries carbonatées du Jurassique moyen de Bourgogne. Thèse d'état, Orsay, 450 pp.
Purser, B.H., 1980. Sédimentation et diagenèse des carbonates néritiques récents, Tome 1. Technip. 366 pp.
Purser, B.H., 1983. Sédimentation et diagenèse des carbonates néritiques récents, Tome 2. Technip. 389 pp.
Purser, B.H., 1989. Plates-formes carbonatées exemple du Jurassique moyen du Bassin de Paris, Dynamique et méthodes d'étude des bassins sédimentaires. Technip, pp. 145–164.
Riboulleau, A., Baudin, F., Daux, V., Hantzpergue, P., Renard, M., Zakharov, V., 1998. Evolution de la paléotempérature des eaux de la plate-forme russe au cours du Jurassique supérieur. Comptes Rendus de l'Académie des Sciences 326, 239–246.
Robin, C., Guillocheau, F., Allemand, P., Bourquin, S., Dromart, G., Gaulier, J.M., Prijac, C., 2000. Time and space-scales of the tectonic control of a flexural intracratonic basin: the Paris Basin. Bulletin de la Société géologique de France 171, 181–196.
Roche, D.M., Donnadieu, Y., Pucéat, E., Paillard, D., 2006. Effect of changes in delta O-18 content of the surface ocean on estimated sea surface temperatures in past warm climate. Paleoceanography 21.
Roduit, N., 2008. JMicroVision: image analysis toolbox for measuring and quantifying components of high-definition images.
Schlager, W., 1993. Accommodation and supply—a dual control on stratigraphic sequences. Sedimentary Geology 86, 111–136.
Schlager, W., 2005. Carbonate sedimentology and sequence stratigraphy, 8. SEPM Concepts in Sedimentology and Paleontology. 200 pp.
Sellwood, B.W., Scott, J., Mikkelsen, P., Akroyd, P., 1985. Stratigraphy and sedimentology of the Great Oolite Group in the Humbly Grove Oilfield, Hampshire. Marine and Petroleum Geology 2, 44–55.
Shackleton, N.J., Kennett, J.P., 1975. Paleotemperature history of the Cenozoic and initiation of Antarctic glaciation: oxygen and carbon isotope analyses in DSDP sites 277, 279 and 289. Initial Reports of the Deep Sea Drilling Project 29, 743–755.
Steuber, T., Rauch, M., Masse, J.P., Graaf, J., Malkoc, M., 2005. Low-latitude seasonality of Cretaceous temperatures in warm and cold episodes. Nature 437, 1341–1344.
Surlyk, F., 1991. Sequence stratigraphy of the Jurassic lowermost Cretaceous of East Greenland. American Association of Petroleum Geologists Bulletin 75, 1468–1488.
Thierry, J., 2000. Late Sinemurian, Middle Toarcian, Middle Callovian, Early Kimmeridgian, Early Tithonian. In: Crasquin, S. (Ed.), Atlas Peri-Tethys, Palaeogeographical maps—Explanatory notes. CCGM/CGMW Édit, Paris, pp. 49–110.
Thierry, J., Cariou, E., Dubois, P., Fily, G., Gabilly, J., Laurin, B., Le Roux, J., Lorenz, J., Rioult, M., Yapaudjian, L., 1980. Jurassique moyen. Synthèse géologique du Bassin de Paris: In: Mégnien, C., Mégnien, F. (Eds.), Stratigraphie et paléogéographie. BRGM. 101, vol. I, pp. 125–193.
Thierry, J., Marchand, D., Fortwengler, D., Bonnot, A., Jardat, R., 2006. Les ammonites du Callovien–Oxfordien des sondages Andra dans l'Est du bassin de Paris: synthèse biochronostratigraphique, intérêts paléoécologique et paléobiogéographique. Comptes Rendus Geosciences 338, 834–853.
Tucker, M.E., Wright, V.P., 1990. Carbonate Sedimentology. Blackwell Science, Oxford. 482 pp.
Vail, P.R., Mitchum, R.M., Thompson, S., 1977. Seismic stratigraphy and global changes of sea level. Part 3 Relative changes of sea level from coastal onlap. Seismic stratigraphy. In: Payton, C. (Ed.), Memoir, vol. 26. American Association of Petroleum Geologists, pp. 63–81.
Vidier, J.P., Garcia, J.P., Thierry, J., Fauconnier, D., 1995. The Dogger of the Boulonnais (Northern Paris Basin)—new chronological and sequence stratigraphic framework of the Jurassic carbonate formations on the margin of the London-Brabant Massif. Comptes Rendus de l'Académie des Sciences Serie II Fascicule a-Sciences de la Terre et des Planètes 320, 219–226.
Weissert, H., Mohr, H., 1996. Late Jurassic climate and its impact on carbon cycling. Palaeogeography, Palaeoclimatology, Palaeoecology 122, 27–43.
Wierzbowski, H., 2002. Detailed oxygen and carbon isotopic stratigraphy of the Oxfordian in Central Poland. International Journal of Earth Sciences 91, 304–314.
Wierzbowski, H., 2004. Carbon and oxygen isotope composition of Oxfordian–Early Kimmeridgian belemnite rostra: palaeoenvironmental implications for Late Jurassic seas. Palaeogeography, Palaeoclimatology, Palaeoecology 203, 153–168.
Wierzbowski, H., Joachimski, M., 2007. Reconstruction of late Bajocian–Bathonian marine palaeoenvironments using carbon and oxygen isotope ratios of calcareous fossils from the Polish Jura Chain (central Poland). Palaeogeography, Palaeoclimatology, Palaeoecology 254, 523–540.
Wierzbowski, H., Joachimski, M.M., 2009. Stable isotopes, elemental distribution, and growth rings of Belemnopsid belemnite rostra: proxies for belemnite life habitat. Palaios 24, 377–386.
Zachos, J.C., Stott, L.D., Lohmann, K.C., 1994. Evolution of early Cenozoic marine temperatures. Paleoceanography 9, 353–387.